Global chemical transport model study of ozone response to changes in chemical kinetics and biogenic volatile organic compounds emissions due to increasing temperatures: Sensitivities to isoprene nitrate chemistry and grid resolution

Akinori Ito,[1] Sanford Sillman,[2] and Joyce E. Penner[2]

[1] Global modeling studies show a wide variability in the response of the O_3 budget to climate change as projected by applying Intergovernmental Panel on Climate Change scenarios in climate models. We employ sensitivity studies to elucidate the major uncertainties in the response of tropospheric O_3 to perturbations in biogenic volatile organic compounds (BVOC) emissions and reaction rate coefficients due to changes in temperature. The change in global O_3 burden due to an increase in BVOC emissions associated with a +5 K depends critically on the assumed treatment for the fraction of NO_x recycled (0–100%) from isoprene nitrate (+9 to +34 Tg), in contrast to the chemical reaction rate coefficients response (−8 to −9 Tg). The model O_3 burden shows sensitivity (40 Tg) to the NO_x recycling efficiencies (0–100%) similar to the burden's sensitivity to the grid resolution ($4° \times 5°$–$1° \times 1°$). The correlation of O_3 with total alkyl nitrates (ΣANs) in the surface air at a California forest site shows sensitivity to the NO_x recycling (40–100%) similar to the correlation's sensitivity to the horizontal resolution ($4° \times 5°$–$1° \times 1°$). The results of the sensitivity simulations imply that the slope of O_3 to ΣANs might be used to constrain the yield of isoprene nitrate and NO_x recycling fraction, but better agreement could be achieved by using a higher-resolution model with even higher NO_x recycling from isoprene nitrate. Our results suggest that the reduction of NO_x recycling from isoprene nitrate be set apart from that due to the effect of the grid resolution in the chemical transport model.

1. Introduction

[2] A number of global modeling studies have suggested that projected climate changes over the next century will result in a decrease in the overall global tropospheric burden of ozone (O_3) because of the increased destruction of O_3 associated with increased water vapor [e.g., *Brasseur et al.*, 1998; *Johnson et al.*, 1999; *Stevenson et al.*, 2000; *Dentener et al.*, 2006a]. *Stevenson et al.* [2006] have intercompared a total of 26 different global atmospheric chemistry models. Simulations for the assessment included the influence of climate change from 2000 and 2030 with global annual mean surface temperatures of between 0.31 and 0.95 K projected by applying Intergovernmental Panel on Climate Change (IPCC) scenarios in climate models. The models show a wide variability in the response of the global tropospheric O_3 budget when a climate change scenario is considered. These differences highlight significant imperfections in our current understanding of the key factors involved (e.g., deep tropical convection, stratosphere-troposphere exchange, and water vapor response).

[3] Several 3-D chemical transport model (CTM) sensitivity studies have been performed to elucidate the major uncertainties in the response of O_3 to climate change. *Wild* [2007] and *Wu et al.* [2007] have demonstrated that the magnitudes of the emissions of nitrogen oxides ($NO_x = NO + NO_2$) from lightning and of isoprene emissions from vegetation contribute to major uncertainties in model calculations of O_3 production. Both of them recognized that the different isoprene chemistry schemes might be an important source of differences between model studies. Our 3-D model study follows these comprehensive studies and aims to elucidate the role of the organic hydroxynitrates ($RONO_2$, "isoprene nitrates") from biogenic volatile organic compounds (BVOC) emissions in the response of O_3 to temperature increases.

[4] There has been increasing attention paid to the climate change penalty of an increase in surface O_3 mixing ratios

---

[1]Frontier Research Center for Global Change, Japan Agency for Marine-Earth Science and Technology (JAMSTEC), Yokohama, Japan.
[2]Department of Atmospheric, Oceanic, and Space Sciences, University of Michigan, Ann Arbor, Michigan, USA.

near polluted areas. However, regional and global model studies have shown that there are significant uncertainties in the response of surface O_3 to temperature increases, especially over the southeastern United States [*Hogrefe et al.*, 2004; *Murazaki and Hess*, 2006; *Dawson et al.*, 2007; *Tagaris et al.*, 2007; *Racherla and Adams*, 2008; *Wu et al.*, 2008; *Zhang et al.*, 2008]. *Dawson et al.* [2007] used the CBM-IV chemical mechanism [*Gery et al.*, 1989] and showed that a uniform increase of surface temperature by 2.5 K would result in $0-4$ ppb increases of the summertime daily maximum 8-h average O_3. *Hogrefe et al.* [2004] used the CBM-IV chemical mechanism and found the average daily maximum 8-h O_3 increase of $4-8$ ppb during summertime in the 2050s relative to the 1990s using the IPCC SRES A2 scenario (1.5–3.5 K). *Zhang et al.* [2008] reported a lower O_3 increase of $1-5$ ppb using the IPCC A1B scenario (2–4.6 K). *Racherla and Adams* [2008] used 100% NO_x recycling with a 12% yield of isoprene nitrate [*Horowitz et al.*, 1998] and predicted a 5 ppb increase in the 95th percentile O_3 in response to the 1.4-K increase in the surface temperatures projected using the IPCC SRES A2 scenario. *Murazaki and Hess* [2006] used 100% NO_x recycling with an 8% yield [*Horowitz et al.*, 2003] without considering changes in BVOC emissions and reported a smaller average O_3 increase of $1-2$ ppb during summertime between 1991 and 1999 and 2091–2099 using the IPCC A1B scenario (2–3.5 K) than the $3-9$ ppb range reported by *Racherla and Adams* [2006]. On the other hand, *Tagaris et al.* [2007] and *Wu et al.* [2008] found little effect. *Wu et al.* [2008] speculated that different treatments of isoprene nitrate chemistry could be a major source of the difference in the model responses of the O_3 to temperature increase. However, *Tagaris et al.* [2007] used the SAPRC mechanism [*Carter*, 2000], in which the NO_x recycling is larger than that in the CBM-IV. Thus the attribution of the differences in the projected O_3 changes to one single factor is often disturbed by multiple competing effects such as the model inputs (e.g., emissions, land cover, and boundary conditions), the BVOC emission models used, the treatments of various atmospheric meteorological and chemical processes in global versus regional models and the horizontal grid resolutions used in the simulations.

[5] There is notable uncertainty in present-day estimates of BVOC emissions. *Guenther et al.* [2006] developed an emissions model to estimate the range of global isoprene emissions. They found that their estimates ranged from 440 to 660 TgC a^{-1} and were strongly dependent on the driving variables, which included land cover (leaf area index and plant functional type distributions) and weather (solar radiation, air temperature, humidity, wind speed, and soil moisture) conditions. A wide range of biogenic emissions for isoprene has been used in different chemistry transport models (220–630 TgC a^{-1} [*Stevenson et al.*, 2006]). The lowest value for isoprene emissions was used for the IPCC Third Assessment Report (TAR) [*Prather et al.*, 2003], while significantly higher emissions were used for the Fourth Assessment Report (AR4). There is an ongoing debate about the convergence toward a common estimate of global isoprene emissions [*Arneth et al.*, 2008; *Lelieveld et al.*, 2008].

[6] Accurate future predictions of isoprene emissions are also uncertain, because the response of terrestrial ecosys-

tems to human activities and climate change is highly complex. Predicted estimates of global isoprene emissions range from 640 to 890 TgC a^{-1} at the end of the 21st century [*Sanderson et al.*, 2003; *Lathière et al.*, 2005; *Wiedinmyer et al.*, 2006], with the biggest driver being the projected increase in surface temperature. *Guenther et al.* [2006] estimated that isoprene emissions may increase by more than a factor of 2 using temperature distributions simulated by applying IPCC A1 scenarios in global climate models for the year 2100. In addition to the temperature changes, the long-term prediction of isoprene emissions is sensitive to land-use change [*Lathière et al.*, 2006; *Ito et al.*, 2008], CO_2 concentration [*Rosenstiel et al.*, 2003; *Arneth et al.*, 2007], and water availability [*Pegoraro et al.*, 2005; *Müller et al.*, 2008].

[7] The spatial and temporal changes of surface O_3 in response to an increase of isoprene emissions due to increased surface temperatures are strongly influenced by background NO_x levels [e.g., *Sanderson et al.*, 2003; *Hauglustaine et al.*, 2005; *Brasseur et al.*, 2006; *Wiedinmyer et al.*, 2006; *Tao et al.*, 2007; *Kunkel et al.*, 2008; *Zeng et al.*, 2008]. In a comprehensive modeling study, *Sillman and Samson* [1995] described how the partitioning of total reactive nitrogen (NO_y) into total peroxy nitrates (ΣPNs), total alkyl nitrates (ΣANs), and HNO_3 is expected to vary as a function of temperature. From their study of polluted rural environments, they concluded that O_3 mixing ratios increase with temperature because of an increase in the thermal decomposition rate for ΣPNs, making ΣANs the dominant contributors to NO_z (= $NO_y - NO_x$) at higher temperatures rather than HNO_3. Their model result was consistent with observations at a rural site in the southeastern United States [*Olszyna et al.*, 1997]. On the other hand, *Day et al.* [2008], who observed atmospheric reactive nitrogen compounds at a California forest site, argued that there was a larger increase in the contribution of HNO_3 to NO_z with temperature and a smaller increase in the contribution of ΣANs to NO_z than that calculated by *Sillman and Samson* [1995]. They attributed the inconsistency between the model and observation to a steep increase in the hydroxyl radical (OH) inferred from the observations of temperature trends in the HNO_3/ NO_2 ratio. These observed changes in reactive nitrogen compounds versus temperature provide a good basis for evaluating the ability of models to predict temperature-dependent responses. The temperature-dependent response of NO_y partitioning is especially important for assessments of future O_3, because the fate of NO_x significantly affects O_3 formation in the global atmosphere. Thus it is meaningful to compare the sensitivity of relatively long lived NO_x reaction products (ΣPNs, ΣANs and HNO_3) in a CTM to temperature changes with those observed.

[8] Previous box and 3-D model studies on regional and global scales have demonstrated that O_3 mixing ratios and reactive nitrogen partitioning are sensitive to uncertainties in the chemical oxidation pathways of isoprene [e.g., *Horowitz et al.*, 1998, 2007; *Pöschl et al.*, 2000; *von Kuhlmann et al.*, 2004; *Fiore et al.*, 2005; *Ito et al.*, 2007a]. *Fiore et al.* [2005] showed that the modeled response of O_3 over the eastern United States to changes in isoprene emissions depends on the fate of isoprene nitrates. The reaction of isoprene nitrates with OH and O_3

can lead to the net production of NO_x (recycling) in the remote atmosphere or to the loss of NO_x in isoprene-rich air if there are significant yields of secondary multifunctional organic nitrates [*Giacopelli et al.*, 2005]. In an extreme case, when the recycling of NO_x was changed from 0% to 100%, surface O_3 mixing ratios increased by approximately 20% at almost all locations [*Ito et al.*, 2007a], which was comparable to the difference between different chemical mechanisms considered in the box model intercomparison by *Pöschl et al.* [2000].

[9] *Day et al.* [2003] found that the ΣANs is strongly correlated with O_3 with a slope of 80 O_3 per ΣANs (ppb/ ppb) at UC–BFRS. *Horowitz et al.* [2007] used measurements from the ICARTT field campaign [*Fehsenfeld et al.*, 2006; *Singh et al.*, 2006] to infer the yield of isoprene nitrate and the NO_x recycling fraction, based in part on the model versus measured slope (82 observed, 81 simulated with 40% NO_x recycling and a 4% yield of isoprene nitrate). Recently, *Paulot et al.* [2009] found a higher yield (12%) and recycling efficiency of 55% on the basis of an analysis using atmospheric smog chamber experiments. *Perring et al.* [2009] suggested much higher recycling efficiencies for different yields (67% isoprene nitrates recycling for 12% yield; 97% for 4.4%) on the basis of an observed correlation between ΣANs and HCHO. We investigate the sensitivity of O_3 per ΣANs for different NO_x recycling fractions to understand why the NO_x recycling fraction obtained by the model calibration is lower than that obtained by *Paulot et al.* [2009].

[10] In addition to the effects of the treatment of isoprene chemistry, the production of O_3 over isoprene-emitting regions near polluted areas is influenced by the model resolution, owing to artificial mixing of air masses of different origins when near surface emissions are added to coarse grids [e.g., *Sillman et al.*, 1990; *Liang and Jacobson*, 2000; *Fiore et al.*, 2003; *Wild and Prather*, 2006; *Wild*, 2007]. *Sillman et al.* [1990] calculated more O_3 production in the boundary layer and less NO_z export to the free troposphere (FT) at lower resolution, because dilution of precursor NO_x emissions in a coarse model grid increased the O_3 production efficiency, defined as the number of O_3 molecules produced per unit NO_x oxidized [*Liu et al.*, 1987]. *Fiore et al.* [2003] compared the GEOS-Chem model with regional model simulations (horizontal resolution of 36 km^2) and showed that the $4° \times 5°$ resolution captured the large-scale features of the surface O_3 distribution, although the ability to capture local O_3 maxima was compromised.

[11] The purpose of this paper is to investigate the processes that could have a major impact on O_3 mixing ratios when temperatures change. We focus on the link between the treatment of isoprene nitrates and the horizontal resolution in the model and on the evaluation of the model predictability of temperature-dependent responses of O_3 and the relatively long lived reactive nitrogen compounds. For this purpose, a global CTM is used to calculate the O_3 mixing ratios. We investigate a sensitivity study, in which we prescribe the water vapor concentration in the model and only perturb the effects of temperature on chemical reaction rates and BVOC emissions. We also examine the correlation between O_3 and temperature and between reactive nitrogen species and temperature in the day-to-day record as predicted by the CTM and in comparison with observations

over an isoprene-emitting region (reported by *Day et al.* [2008]). These day-to-day correlations with temperature can reflect the influence of a wide variety of meteorological factors (solar radiation, humidity, mixed layer depth, and transport patterns), which coincidentally vary with temperature, rather than the effect of temperature in isolation. Day-to-day correlations with temperature also may not reflect the combined changes in meteorology and emissions associated with future climate. Nonetheless, they provide a test of the ability of models to predict changes in chemically reactive species in response to temperature against ambient conditions. Section 3 describes the different scenarios examined. Section 4 examines the sensitivity of the global O_3 budget and surface mixing ratios in different simulations as well as comparisons of the model with observations of O_3 and other intermediate species. Section 5 presents a summary of our findings.

2. Model Approach

[12] For this study, we use the Integrated Massively Parallel Atmospheric Chemical Transport (IMPACT) model driven by assimilated meteorological fields which are obtained from the Goddard Earth Observation System (GEOS) of the NASA Global Modeling and Assimilation Office (GMAO) [*Schubert et al.*, 1993]. The GEOS-3 meteorological data set [*Zhu et al.*, 2003] for the year 2001 is suitable for the comparison with the observations by *Day et al.* [2008]. IMPACT was originally developed at the Lawrence Livermore National Laboratory (LLNL) [*Rotman et al.*, 2004] but was extended to treat aerosols and detailed chemical reactions for a wider set of VOC at the University of Michigan [*Liu et al.*, 2005; *Feng and Penner*, 2007; *Ito et al.*, 2007a]. The GEOS-3 meteorological fields were provided with a 6-h temporal resolution on a horizontal resolution of $1° \times 1°$ with 48 vertical layers. Since the gas-phase model does not communicate with the aerosol model interactively, two separate simulations were performed for a 1-year time period with a 6-month spin-up period for the gas-phase model and a 2-month spin-up for the aerosol model.

[13] A number of revisions to the chemistry described by *Ito et al.* [2007a] were made for the present study. We adopt the production of secondary multifunctional organic nitrates (XNITR) from the oxidation of isoprene and terpene nitrates by the three main oxidants, OH, O_3, and NO_3 in the work of *Horowitz et al.* [2007] to the previous IMPACT mechanism of *Ito et al.* [2007a]. Our yield of isoprene nitrate from the reaction of isoprene peroxy radicals with NO which ranges from 8% for 593 hPa to 12% for 1000 hPa [*Sprengnether et al.*, 2002] is larger than the 4% yield [*Chen et al.*, 1998] in the base simulation of *Horowitz et al.* [2007]. This chemistry reaction mechanism assumes that the reaction of isoprene nitrate with OH and O_3 yields

$$A \times (GLYC + NO_2) + B \times (XNITR) + (HO_2), \qquad (1)$$
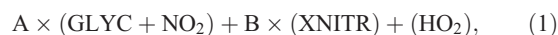
where GLYC represents hydroxyacetaldehyde, sum of A and B equals 1, and A takes on the values 0, 0.4, and 1. We changed the production of hydroxyacetone in the assumption by *Paulson and Seinfeld* [1992] to GLYC, on the basis of the model comparison with observations of *Ito et al.*

Table 1. Global Emissions of O_3 Precursors Except Biogenic Volatile Organic Compounds for the Year 2001[a]

Species	Emission Rate
NO_x	46
CO	1232
Methylethyl ketone	8.6
C_2H_6	9.0
C_3H_8	4.5
CH_3CHO	6.0
HCHO	6.1
C4−C5 alkanes (ALK4)	15.9
$\geq$C6 alkanes (ALK7)	10.3
Ethene	14.4
Propene	18.9
Trans-2-butene	5.1
Benzene	7.2
Toluene	10.0
m-xylene	9.1
Acetone	4.4
Methanol	11.1
Formic acid	2.4
Acetic acid	14.7
Phenol	12.5

[a]Units are TgN a^{-1} for NO_x, TgCO a^{-1} for CO, and TgC a^{-1} for nonmethane volatile organic compounds.

[2007a]. Species scavenging depends on solubility through the Henry's law coefficient, as described by *Rotman et al.* [2004]. The Henry's law constant of 1.7×10^4 M atm^{-1} for isoprene nitrate [*O'Sullivan et al.*, 1996] is of the same order of magnitude as that of 8.3×10^4 M atm^{-1} for HNO$_3$ [*Schwartz and White*, 1981]. XNITR is removed by wet and dry deposition at the same rates as isoprene nitrate, as its further reactions are assumed to convert it to more highly substituted organic nitrates that do not recycle NO$_x$ back into the atmosphere. We include methanol deposition following *Jacob et al.* [2005]. The water vapor in the troposphere is prescribed by the meteorological data. The tropopause height is defined as the lowest level at which a synthetic O$_3$ tracer from the stratosphere is greater than 150 ppbv [*McLinden et al.*, 2000]. Reaction rates are taken from the recent IUPAC [*Atkinson et al.*, 2004] and JPL [*Sander et al.*, 2006] assessments. The aerosols used in the calculation of the uptake of N$_2$O$_5$ are calculated using the model described by *Feng and Penner* [2007]. We apply the same monthly averaged NO$_x$ emission rates and the HO$_x$ (= OH + HO$_2$) and O$_3$ output from an initial gas-phase run with the previously fixed aerosol concentrations for the reaction of N$_2$O$_5$ on aerosols in the aerosol simulation. We use the aerosol emissions of *Dentener et al.* [2006b]. The uptake rates of N$_2$O$_5$, HO$_2$, NO$_2$ and NO$_3$ by aerosols are calculated from the aerosol simulation driven by the 2001 meteorological fields at $2° \times 2.5°$ resolution.

[14] The emissions inventory has been recompiled to represent the year 2001 for the comparison with the measurements by *Day et al.* [2008]. Table 1 lists the global emissions of O$_3$ precursors except BVOC used in the present work. Isoprene emissions are based on a modified version of the inventory of *Guenther et al.* [1995] by *Wang et al.* [1998] and *Bey et al.* [2001]. Monoterpene emissions are based on the work of *Guenther et al.* [1995] as modified by *Wang et al.* [1998]. The BVOC emissions are calculated interactively with the same meteorological data. We run the model for 1 year and calculate the monthly emissions. Then, we scale the monthly emissions to normalize to a global

biogenic isoprene source of 500 TgC a^{-1} and terpene sources of 130 TgC a^{-1} as in the work of *Guenther et al.* [1995] for all scenarios at the base case temperature. The other temperature-dependent BVOC emissions for ethene, propene, acetone, and methanol are distributed according to emissions of isoprene [*Ito et al.*, 2007a]. We use the surface air temperature dependency from *Guenther et al.* [1999] following *Palmer et al.* [2006] to determine the resulting change in emissions. This functional dependence exponentially increases BVOC emissions with increasing surface air temperature up to a maximum that is dependent on the average temperature during the past 15 days. Lightning NO$_x$ emissions are based on the convective mass fluxes from the meteorological fields at each resolution [*Allen and Pickering*, 2002]. The vertical distribution of the source is based on observed profiles [*Pickering et al.*, 1998]. We normalized the total emissions to 3 TgN a^{-1} as per *Bey et al.* [2001]. The soil NO$_x$ emissions are obtained from *Yan et al.* [2005] for the year 2001. Anthropogenic fossil fuel emissions are taken from M. G. Schultz et al. (RETRO emission data sets and methodologies for estimating emissions, project report, 2007, available at http://retro.enes.org/reports/D1-6_final.pdf) for 2000 except for aircraft NO$_x$ emissions, which are from the monthly mean emission inventory for 1999 of *Mortlock and Van Alstyne* [1998] and *Sutkus et al.* [2001]. The global biomass burning emissions are updated to those of *Ito et al.* [2007b], which are based on the emissions developed by *Ito and Penner* [2005] for the year 2000 and scaled to the year 2001 using the TOMS AI data [*Herman et al.*, 1997]. The MODIS fire product [*Giglio et al.*, 2006] is used to produce the seasonal variations in open biomass burning emissions except in southern Africa, where regional emissions from open vegetation burning are available [*Ito et al.*, 2007c].

3. Chemical Transport Model Sensitivity Studies

[15] The different simulations performed in this study are summarized in Table 2. To assess the effects of increases in temperature on the chemical composition of the atmosphere, we consider the change in both the reaction rate coefficients (section 3.1) that depend on temperature and the BVOC emissions (section 3.2) to perturbations of temperature throughout the troposphere. A fixed uniform change of temperature is useful to investigate each of these parameters separately so that the effects of each as well as the synergy can be determined. This would help identify the major factors that could have an effect on air quality as temperature changes. To assess the uncertainties in the model response, we examine the sensitivity of O$_3$, its precursors, and its production to the treatment of the recycling of NO$_x$ from isoprene nitrates (section 3.3) and to the model resolution (section 3.4).

3.1. Effects of Temperature on Chemistry

[16] The effects of temperature on oxidant photochemistry are examined by applying globally uniform changes in temperature (±5 K) to the chemical reaction rate coefficients only after *Wild* [2007]. Increased temperatures affect chemical reaction kinetics and thus O$_3$ production and loss rates. The reactions responsible for this temperature effect are mainly associated with the chemistry of peroxyalkyl nitrates

Table 2. Summary of Different Simulations Performed in This Study

Simulation	Run Name	Isoprene Emission	NO$_x$ Recycling, %	Resolution
1	L^a_0	500	0	4° × 5°
2	L_40	500	40	4° × 5°
3	L_100	500	100	4° × 5°
4	L_0_P^{b}E^c	940	0	4° × 5°
5	L_0_M^{d}E	270	0	4° × 5°
6	L_40_PE	940	40	4° × 5°
7	L_40_ME	270	40	4° × 5°
8	L_100_PE	940	100	4° × 5°
9	L_100_ME	270	100	4° × 5°
10	L_0_PC^e	500	0	4° × 5°
12	L_0_MC	500	0	4° × 5°
13	L_40_PC	500	40	4° × 5°
13	L_40_MC	500	40	4° × 5°
14	L_100_PC	500	100	4° × 5°
15	L_100_MC	500	100	4° × 5°
16	L_0_PEC^f	940	0	4° × 5°
17	L_0_MEC	270	0	4° × 5°
18	L_40_PEC	940	40	4° × 5°
18	L_40_MEC	270	40	4° × 5°
19	L_100_PEC	940	100	4° × 5°
20	L_100_MEC	270	100	4° × 5°
21	M^g_40	500	40	2° × 2.5°
22	H^h_40	500	40	1° × 1°
23	H^h_100	500	100	1° × 1°

[a]Low resolution (4° × 5°).
[b]Temperature increase (+5 K) applied to chemical reaction rate coefficients and/or biogenic volatile organic compound (BVOC) emissions.
[c]BVOC emission perturbation.
[d]Temperature decrease (−5 K) applied to chemical reaction rate coefficients and/or BVOC emissions.
[e]Chemical reaction rate coefficient perturbation.
[f]BVOC emission and chemical reaction rate coefficient perturbations.
[g]Middle resolution (2° × 2.5°).
[h]High resolution (1° × 1°).

such as peroxyacetyl nitrate (PAN, $CH_3C(O)O_2NO_2$), because thermal decomposition is the main loss reaction for these compounds [*Carter et al.*, 1979]. Although we focus on the sensitivity of O$_3$ in this paper, we note that the sensitivity of CH$_4$ oxidation to temperature has also been shown to have temperature dependence relevant for chemistry-climate links [*Johnson et al.*, 1999; *Fiore et al.*, 2006].

3.2. Effects of Temperature on Emissions

[17] The effects of temperature on BVOC emissions are examined by applying a perturbation based on changes in temperature (±5 K) to the calculation of BVOC emission rates. The BVOC whose emission is sensitive to temperature include isoprene, ethene, propene, terpenes, acetone, and methanol. Our estimates of isoprene emission range from 270 (−5 K) to 940 TgC a^{-1} (+5 K). In section 4.1.3, we discuss the implications of the findings from recent studies by *Arneth et al.* [2007] and *Heald et al.* [2009].

3.3. Effects of NO$_x$ Recycling From Isoprene Nitrates

[18] The response of O$_3$ to a change in temperatures is sensitive to the NO$_x$ recycling rate from the oxidation products of biogenic emissions, which are related to the temperature. The treatment of the recycling of NO$_x$ when isoprene nitrates and nitrates from the oxidation of terpene react with OH and O$_3$ is varied from 0% to 40% to 100% following *Horowitz et al.* [2007].

3.4. Effects of Model Resolution

[19] The response of O$_3$ to the NO$_x$ recycling rate is influenced by the model resolution when biogenic emissions are mixed with anthropogenic sources within the same coarse grids. We examine the sensitivity of O$_3$, its precursors, and its production to horizontal resolution by running the model at three different horizontal resolutions: low resolution (4° × 5°), middle (2° × 2.5°), and high (1° × 1°). The middle and high resolutions used here may be comparable with those used by *Wild and Prather* [2006] at T42 (2.8° × 2.8°) and T106 (1.1° × 1.1°) resolution for March and April 2001.

4. Model Results and Discussion

4.1. Global Ozone Budget

[20] The results of the sensitivity studies for the low-resolution simulations (numbers 1–20) listed in Table 2 are shown in Figure 1. In the analysis of the global O$_3$ budget, "O$_3$" represents "O$_3$ + NO$_2$ + 2 × NO$_3$ + PAN + MPAN + HNO$_4$ + HNO$_3$ + 3 × N$_2$O$_5$ + npan." The lifetime of O$_3$ is determined from its chemical removal and deposition rates. In sections 4.1.1 and 4.1.2, we investigate each of these parameters separately. In section 4.1.3, we examine the combined effect of these parameters. In section 4.1.4, we explore the sensitivity to model resolution.

4.1.1. Sensitivities to BVOC Emissions and NO$_x$ Recycling

[21] The response of the calculated O$_3$ budget to the perturbation of BVOC emissions due to temperature changes is sensitive to the treatment of the recycling of NO$_x$. Increased recycling of NO$_x$ from isoprene nitrates provides a direct increase in the model mixing ratios of both NO$_x$ and organics (which are also recycled), which lead to increased O$_3$ formation and thus its burden from 330 Tg for (L_0) to 370 Tg for (L_100). Higher NO$_x$ recycling could transport more NO$_x$ to remote regions than lower recycling, because the former does not remove NO$_x$ efficiently over isoprene-emitting regions (see section 4.2 for further discussion).

[22] *Stevenson et al.* [2006] showed the large spread in O$_3$ burden (274–407 Tg) among 25 atmospheric models, although it is not clear how many previous studies have included the isoprene nitrate chemistry. *Wild* [2007] did not include isoprene nitrates in the simplified hydrocarbon oxidation scheme and showed that differences in isoprene emissions (220–630 TgC a^{-1}) might account for 20 Tg in O$_3$ burden. *Wu et al.* [2008] used 0% NO$_x$ recycling with the yield of *Sprengnether et al.* [2002] and showed little changes in O$_3$ burden (315–319 Tg) by varying the isoprene emissions (0–400 TgC a^{-1}). The effect of increased isoprene emissions from 270 to 940 TgC a^{-1} on the increase in O$_3$ burden depends critically on the assumed treatment for the fraction of NO$_x$ recycled and ranges from 17 Tg for (L_0_PE) − (L_0_ME) to 57 Tg for (L_100_PE) − (L_100_ME). This interrelationship can be explained by the synergy between additional BVOC and increased ambient NO$_x$ associated with recycling [*McKeen et al.*, 1991; *Tao et al.*, 2003]. As BVOC emissions are increased, ambient NO$_x$ in biogenic source regions is increased with increasing NO$_x$ recycling owing to the increase of the organic nitrates except XNITR. The increase
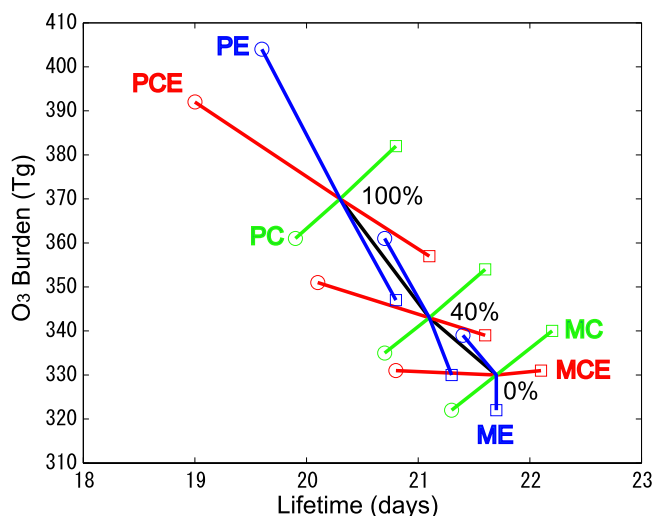
Figure 1. The relationship between the tropospheric burden of O_3 and its lifetime from chemical removal and deposition from the results of the sensitivity studies listed in Table 2. The black line represents the sensitivity to the assumed recycling of NO_x from isoprene nitrates. The red lines denote the sensitivity to changes in both chemical reaction rate coefficients and emissions from changes in temperature. The blue lines indicate the sensitivity to changes in emissions from changes in temperature. The green lines show the sensitivity to changes in chemical reaction rate coefficients from changes in temperature. The circles represent results for a temperature increase (+5 K) applied to the chemistry and/or emissions. The squares represent results for a temperature decrease (−5 K) applied to the chemistry and/or emissions. PC and MC represent temperature increase (+5 K) and decrease (−5 K), respectively, applied to chemical reaction rate coefficients. PE and ME represent temperature increase (+5 K) and decrease (−5 K), respectively, applied to emissions. PCE and MCE represent temperature increase (+5 K) and decrease (−5 K), respectively, applied to chemical reaction rate coefficients and emissions.

in O_3 is driven largely by the increased role of PAN as a transporter of NO_x and the rerelease of NO_x from isoprene nitrates is determined by the recycling fraction of NO_x. This increases the transport of NO_x to the remote troposphere [e.g., *Singh et al.*, 1998, 2000], which increases the overall net production of O_3 because O_3 production in the remote troposphere is more efficient [e.g., *Liu et al.*, 1987].

[23] The slope of the lifetime versus O_3 burden due to the effect of a temperature increase on the BVOC emissions is smaller when the recycling of NO_x is lower. The steeper slope represents a higher chemical production of O_3. Increases in BVOC emissions lead to increased net chemical O_3 production for (L_40_PE) − (L_40) (17 Tg a^{-1}) and (L_100_PE) − (L_100) (58 Tg a^{-1}) recycling of NO_x but decreased net production for (L_0_PE) − (L_0) (−2 Tg a^{-1}). The slope for the low recycling of NO_x due to the effects of a decrease in temperature of −5 K on emissions is steeper than that owing to an increase of +5 K. *Wu et al.* [2007] found that net chemical O_3 production became saturated for nonmethane volatile organic com-

pounds (NMVOC) emissions in the range of 200 and 500 (Tg C a^{-1}). This is consistent with our results. A further increase in the BVOC emissions to 940 (Tg C a^{-1}) changes the sign of the net chemical production. These results indicate that a lower recycling fraction for NO_x introduces a larger chemical loss rate for O_3 for the effect of a temperature increase of 5 K on BVOC emissions. However, the O_3 burden (17 Tg O_3) is increased for (L_0_PE) − (L_0_ME), mainly because the wet deposition of HNO_3 (−13 Tg O_3 a^{-1}) is decreased.

4.1.2. Sensitivity to Chemical Reaction Rate Change due to Temperature Increases

[24] The effect of changes in chemical reaction rates due to increased temperatures by 5 K causes slight decreases (−8 to −9 Tg) in the total tropospheric O_3 burden in our model. Previously, *Sillman and Samson* [1995] suggested that total tropospheric O_3 would decrease in this case because precursors are processed and removed more rapidly in polluted regions, where the O_3 production efficiency per NO_x molecule is lower. *Wild* [2007] showed that the tropospheric burden of O_3 dropped by less than 1% for a temperature rise of 5 K on oxidant photochemistry. Most of the decreases in O_3 are seen in the FT (global averaged differences for (L_40_PC) − (L_40) are −1.1 ppb in FT versus −0.5 ppb in surface air) and remote sites where NO_x from the decomposition of PAN affects O_3 owing to the higher O_3 production efficiency per unit NO_x (OPE) in these regions. On the other hand, the effect of increased temperatures on chemistry leads to increased O_3 in source regions (see section 4.2).

[25] Here, we find that the change in the O_3 burden due to the change in reaction rate coefficients associated with a temperature change is largely independent from the assumed NO_x recycling fraction, in contrast to the BVOC emission response. Gross chemical O_3 production decreases (−13.6 Tg a^{-1}) for (L_40_PC) − (L_40) in response to reduced NO_x (the global averaged differences are −1.8 ppt in the FT versus +1.6 ppt in surface air) resulting from less efficient transport by PAN (as suggested by *Singh et al.* [1998, 2000]). The decrease in chemical O_3 production (−23.4 Tg a^{-1}) for (L_100_PC) − (L_100) is larger than that (−6.7 Tg a^{-1}) for (L_0_PC) − (L_0) in response to larger decrease in NO_x (the global averaged differences in the FT are −2.4 ppt for (L_100_PC) − (L_100) versus −1.4 ppt for (L_0_PC) − (L_0)). However, this is counterbalanced by larger decrease in total loss (−23.5 Tg a^{-1}) for (L_100_PC) − (L_100) than that (−6.5 Tg a^{-1}) for (L_0_PC) − (L_0), which is reflected in larger decrease in the chemical loss via the reaction of O_3 with OH and photochemical destruction (the global averaged differences in the FT are −1.3 ppb for (L_100_PC) − (L_100) versus −0.98 ppb for (L_0_PC) − (L_0)).

4.1.3. Sensitivity to Combined Simulations

[26] The effect of changes in chemical reaction rates due to increased temperatures (+5 K) causes slight decreases in the total tropospheric O_3 burden (−8 to −9 Tg). Increased emissions of BVOC (+5 K), however, lead to increases in O_3 burden (+9 to +34 Tg) and this effect is larger than the net decrease in global O_3 burden. Overall, global mean O_3 increases with temperature (+5 K), ranging from 1 Tg for 0% NO_x recycling to 22 Tg for 100%.

(a) Isoprene

(b) PAN

(c) Nitrogen Oxides
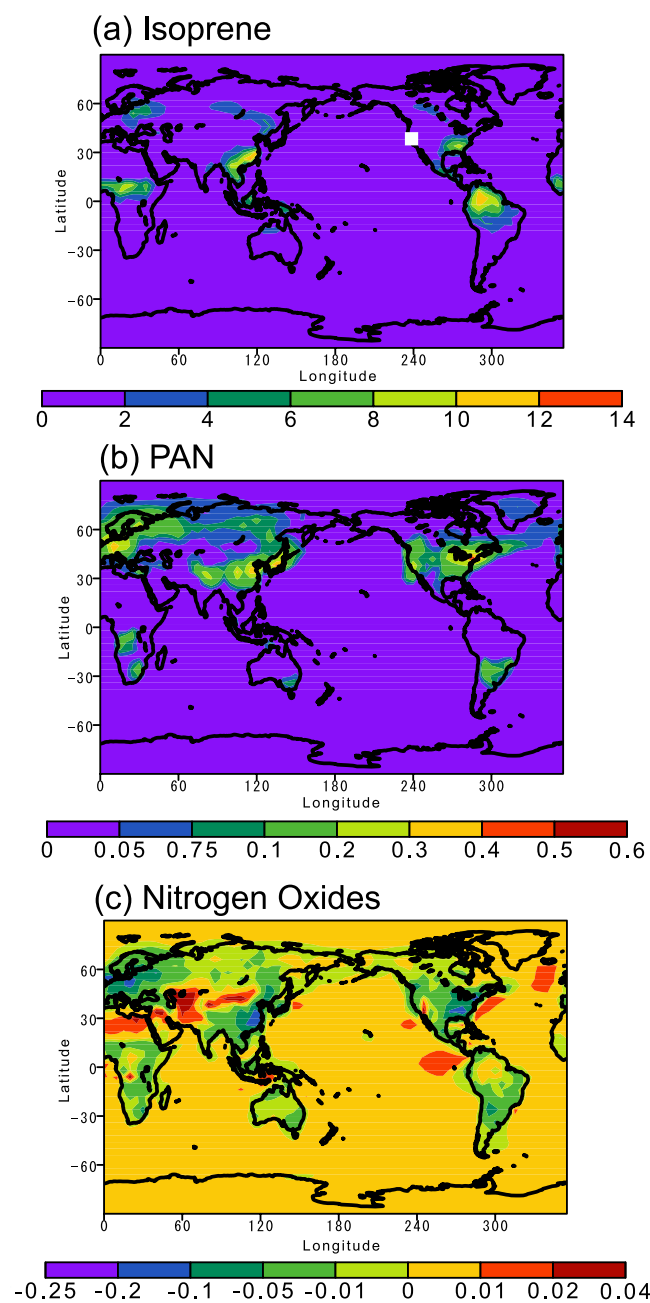
Figure 2. The changes in mixing ratios (ppbv) for (a) isoprene, (b) peroxyacetyl nitrate (PAN), and (c) NO_x, for the difference between the case with increased emissions caused by a 5-K increase in temperature and the base case, (L_40_PE) − (L_40), in the surface air in July. The white box in Figure 2a shows the location of the University of California−Blodgett Forest Research Station (UC−BFRS).

[27] *Arneth et al.* [2007] found that the increase in isoprene emissions induced by temperature and vegetation changes in the next century would be offset when the inhibition of leaf isoprene emissions by increasing atmospheric CO_2 concentration is accounted for in their model. In this case which maintains the isoprene emissions within ±15% of present values, the response of O_3 to temperature increase would be insensitive to the uncertainties in the NO_x recycling rate, because the response of the O_3 burden to the

change in reaction rate coefficients associated with a temperature change is largely independent from the assumed NO_x recycling fraction. Recently, *Heald et al.* [2009] found that future isoprene emissions increased by more than a factor of 2 in 2100 (to 1242 TgC a^{-1}) owing to temperature and vegetation changes even when the effect of CO_2 inhibition is included. In this case, the response of O_3 to future climate would be sensitive to the uncertainties in the NO_x recycling rate, because the increase in global O_3 burden due to an increase in BVOC emissions depends critically on the fraction of NO_x recycled from isoprene nitrate. The divergence of the future predictions of isoprene emissions highlights the need for further study of the effects of changes in isoprene emissions in the future climate.

4.1.4. Sensitivity to Model Resolution

[28] Model results at the low resolution (4° × 5°) which use lower recycling fractions for NO_x (between 0% and 40%) compare better with the tropospheric O_3 burden of 335 ± 10 Tg determined by *Wild* [2007] from available O_3 climatologies. However, the global mean O_3 burden for 2001 is 13% smaller at the high resolution (302 Tg) than at the low with the 40% NO_x recycling fraction (340 Tg), reflecting less net chemical O_3 production at the higher resolution. This amount is comparable to the difference in O_3 burden between 0% and 100% NO_x recycling of isoprene nitrates (40 Tg). The global mean O_3 burden during March and April decreases by 3.0% as the resolution decreases from 2° × 2.5° to 1° × 1°, which is comparable to the decrease (−3.2%) from a resolution change from T42 to T106 calculated by *Wild and Prather* [2006]. On the basis of the tendency calculated using the low-resolution model, the burden is expected to be increased by 8% when 100% recycling of NO_x is assumed rather than 40%. These results suggest that the assumptions of lower BVOC emissions and lower NO_x recycling fractions are not needed for higher-resolution simulation to match the burden of O_3 derived by *Wild* [2007].

4.2. Changes in Surface O_3 and Its Precursors due to Increases in Temperature

[29] The sensitivity of surface O_3 and its precursors to changes in BVOC emissions (section 4.2.1) and chemical reaction rates (section 4.2.2) due to increases in temperature are analyzed here for July. In section 4.2.3, we examine the combined effect of these parameters. In section 4.2.4, we investigate the NO_x recycling fraction associated with model resolution.

4.2.1. Sensitivity to BVOC Emissions

[30] The geographical distribution of the changes in isoprene mixing ratios (ppbv) for (L_40_PE) − (L_40) is shown in Figure 2a. Enhancements of more than 2 ppbv are found over the main isoprene-emitting regions in the temperate and boreal forests. In the tropical forests, the changes reach more than 8 ppbv. The largest changes in tropical forest regions occur because of a large decrease in OH and increase in the photochemical lifetime of isoprene [e.g., *Houweling et al.*, 1998; *Guenther et al.*, 1999]. However, *Lelieveld et al.* [2008] proposed that BVOC oxidation recycles OH efficiently (40−80%) at low-NO_x mixing ratios through reactions of HO_2 with organic peroxy radicals (RO_2), on the basis of the aircraft measurements of OH and related species in unpolluted air over the Amazon

rain forest, laboratory measurements, and numerical modeling. Subsequently, *Butler et al.* [2008] demonstrated that a recycling of OH of 40−50% was needed to match the model results with the observations, although the resulting high-OH concentrations lead to unrealistically low mixing ratios of isoprene. In section 4.3.2.4, the isoprene mixing ratios and OH concentrations from the model results are compared to the observations.

[31] The changes in the PAN mixing ratios (ppbv) are shown for (L_40_PE) − (L_40) in Figure 2b. Increases in the surface PAN mixing ratios are calculated over polluted regions (0.1−0.5 ppbv), reflecting increases in the organic compounds available for the PAN formation.

[32] The change in the NO_x mixing ratio (ppbv) is shown for (L_40_PE) − (L_40) in Figure 2c. Decreases of the surface NO_x mixing ratios (−0.05−0.2 ppbv) are calculated over both the isoprene- and NO_x-emitting regions for the case when 40% recycling fraction for NO_x is assumed. Increases (0.01−0.04 ppbv) are found over remote locations where nitrogen-containing compounds can be transported from the source regions [e.g., *Sanderson et al.*, 2003; *Hauglustaine et al.*, 2005; *Wiedinmyer et al.*, 2006; *Zeng et al.*, 2008]. Increased NO_x is especially noteworthy in the desert and semidesert regions of central Asia and the western United States. In each of these regions there is an apparent release of NO_x imported from neighboring regions that have high emissions of both anthropogenic NO_x and BVOC. These increases in NO_x occur even with the assumed 40% recycling fraction for NO_x. Over the same regions, smaller NO_x increases (up to 0.03 ppbv) occur in the cases with 0% NO_x recycling, while larger NO_x increases (up to 0.09 ppbv) occur in the cases with 100% NO_x recycling.

[33] The resulting changes in surface O_3 mixing ratios due to the effect of a +5-K increase in temperature on emissions are shown for the 0, 40, and 100% recycling fractions for NO_x in Figures 3a−3c. The O_3 changes due to the effects of +5 K on emissions are larger than those due to −5 K (the global averaged differences are 1.3 ppb for (L_40_PE) − (L_40) versus −1.1 ppb for (L_40_ME) − (L_40)), because the responses of O_3 to the temperature changes are subject to the effect of nonlinearities in the BVOC emissions which increase exponentially with increasing surface air temperature.

[34] Decreases in surface O_3 (up to −4.5 ppbv) are found over tropical forests because more isoprene directly reacts with O_3 to increase its loss and more isoprene nitrates act as a sink of NO_x to decrease its production. Under low-NO_x conditions, where O_3 formation is sensitive to the level of NO_x, more NO_x is removed as isoprene nitrates for increased emissions of isoprene as well as other BVOC and more is scavenged as XNITR in the case with a lower recycling fraction for NO_x. The largest increases in surface O_3 (up to 11.4 ppbv) are found near or downwind from polluted areas. These increases occur in two types of locations: (1) source regions in which O_3 formation is likely to be sensitive to VOC emissions, such as over north China and northern Europe, and (2) downwind locations that have increased NO_x (Figure 2c) over the Middle East and central Asia [e.g., *Li et al.*, 2001; *Lelieveld et al.*, 2002; *Wild et al.*, 2004]. Our model results suggest that additional measurements for the downwind regions would be helpful in
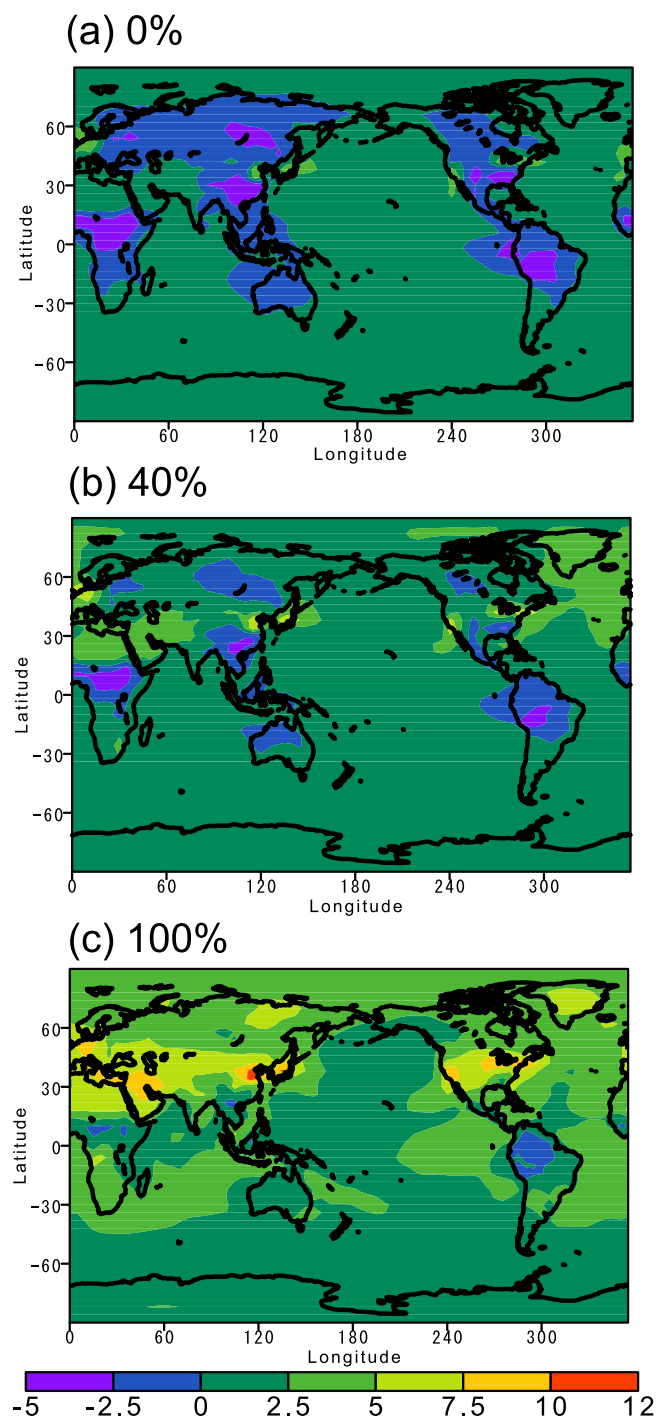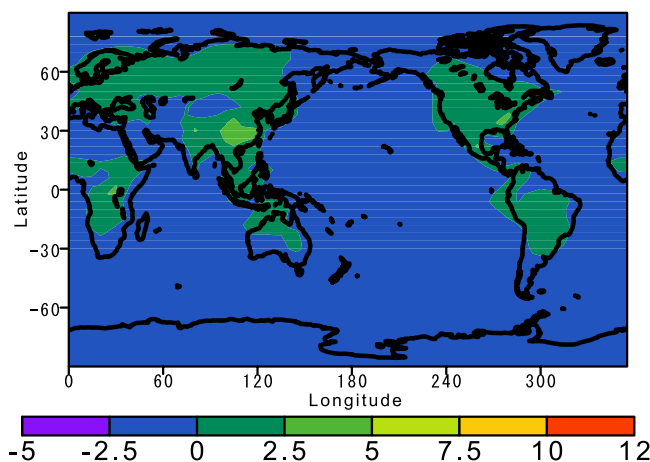

Figure 3. The changes in surface O_3 mixing ratios (ppbv) in July due to the difference between the cases with increased emissions caused by a 5-K increase in temperature (L_0_PE, L_40_PE, and L_100_PE) and the base cases (L_0, L_40, and L_100) for the assumption of (a) 0% recycling of NO_x from isoprene nitrates, (b) 40% recycling of NO_x from isoprene nitrates, and (c) 100% recycling of NO_x from isoprene nitrates.

providing constraints on the temperature response of O_3 and the recycling fraction for NO_x.

[35] The response of O_3 to the effect of increases in temperature on emissions shows that the changes in O_3

Figure 4. The change in surface O_3 mixing ratios (ppbv) in July due to the effects of a 5-K increase in temperature on the chemical reaction rate coefficients (L_40_PC) for the assumption of 40% recycling of NO_x from isoprene nitrates.

are largely determined by the assumed recycling fraction for NO_x. The O_3 increase is larger in the case with higher recycling of NO_x. In the case with 0% recycling of NO_x, O_3 mixing ratios mostly increase (up to 7.3 ppbv) over high-NO_x locations such as Germany, Beijing, Los Angeles, and the New York area. On the other hand, high BVOC emissions regions near polluted areas (e.g., the southeastern United States) result in a decrease in O_3 (up to −4.5 ppbv). This result indicates that the increased BVOC emissions near polluted areas efficiently remove O_3 precursors in the case with lower recycling fractions for NO_x.

[36] *Zhang et al.* [2008] used CMAQ [*Byun and Schere*, 2006] with the CBM-IV chemical mechanism at the horizontal resolution of 36 km and found that the increase in BVOC emissions due to temperature increases caused a decrease in surface O_3 by up to 1 ppb over the southeastern United States. Their results are consistent with our results using a 0% recycling fraction for NO_x. The lumping approach used in the CBM-IV to reduce the complexity of the degradation schemes for higher hydrocarbons is different from that used in this work. A structural lumping, which groups species according to their bond type is used, as opposed to the molecular lumping approach used in this work, where groups of reactions of entire molecules are combined. *Pöschl et al.* [2000] and *von Kuhlmann et al.* [2004] have discussed the differences between these two approaches and attributed the major cause of differences to the approximate 50% loss of carbon in the initial reaction of isoprene with OH in the CBM scheme. Our results suggest that the more likely cause for the decrease in surface O_3 is the implicit assumption of large losses of NO_x in the CBM scheme, which lumps isoprene nitrate into one organic nitrate. The reaction of organic nitrate with OH in the CBM mechanism yields HNO_3 and thus a 0% recycling fraction for NO_x.

4.2.2. Sensitivity of Chemical Reaction Rates to Temperature Increases

[37] The changes in surface O_3 mixing ratios due to the effect of changes in chemical reaction rates associated with temperature increases are shown for the 40% recycling

fraction for NO_x in Figure 4. Surface O_3 increases (up to 4.2 ppbv) with increased temperature at most continental surface locations regardless of the assumed NO_x recycling fraction. The response of O_3 to temperature through changes in the chemical reaction rate coefficients occurs mainly because higher temperatures increase PAN decomposition, and the resulting release of NO_x, HO_x, and organics causes increased O_3 formation [*Carter et al.*, 1979]. *Steiner et al.* [2006] used CMAQ with SAPRC99 chemical mechanism at the horizontal resolution of 4 km and found the average afternoon O_3 increase from 0 to 1 ppb (rural) up to 2−4 ppb (urban) owing to the effect of 2−3 K increase on chemical reaction rates during summertime. This may be comparable to our results over land areas (0−2.5 ppbv) owing to the effect of a 5-K increase on a per-degree basis.

4.2.3. Sensitivity to Combined Simulations

[38] Large uncertainties have been found in the response of surface O_3 over the southeastern United States, when the effects of climate change on isoprene emissions from the biosphere are considered in modeling experiments [e.g., *Hogrefe et al.*, 2004; *Tagaris et al.*, 2007; *Racherla and Adams*, 2008; *Wu et al.*, 2008; *Zhang et al.*, 2008]. Our results show decreases in O_3 (down to −2.5 ppbv) for a 0% NO_x recycling fraction but increases in O_3 (up to 10 ppbv) with a 100% recycling fraction and a uniform 5-K increase in temperature over the southeastern United States (Figure 5).

[39] The rates of increase of O_3 in polluted source regions due to chemistry and emissions are less than 10 ppbv for 0% and 40% NO_x recycling fractions and are 10−14 ppbv for a 100% NO_x recycling fraction, respectively (Figure 5). A similar analysis by *Steiner et al.* [2006] for the San Joaquin Valley in California found an average afternoon O_3 increase of 0−2 ppb in rural locations and 3−5 ppb near urban areas during summertime due to the effect of a 2-K temperature increase on biogenic emissions alone. The SAPRC scheme used by *Steiner et al.* [2006] assigns isoprene nitrate into a lumped organic nitrate with a 65% recycling fraction for NO_x, and thus falls somewhere between our cases with 40% and 100% recycling. Although our results lack the sharp distinction between geographical regions shown by *Steiner et al.* [2006] (who used 4-km horizontal resolution in a regional simulation), our result for California is comparable on a per-degree basis.

4.2.4. Sensitivity to Model Resolution and NO_x Recycling Fraction

[40] The surface O_3 mixing ratios for H_100, L_100, and L_40 in July are compared to investigate the relationship between the change in O_3 due to increases in the horizontal resolution and the change due to the NO_x recycling fractions (Figure 6). The high-ozone region (54−63 ppb) for L_100 is extended further from the source regions to east than that for H_100. Better agreement can be achieved by reducing the NO_x recycling fraction, as shown in L_40. This result illustrates that the treatment of isoprene nitrates as a loss for NO_x in a coarse-resolution model compensates for the higher OPE that occurs in spreading NO_x emissions over a larger box. Thus the lower NO_x recycling fraction inferred in the study by *Horowitz et al.* [2007] than that deduced by *Paulot et al.* [2009] likely includes the effect of horizontal resolution in the model calibration. The lower recycling required at the coarse model grid is probably related to the conversion of NO_2 to HNO_3 in high-OH and low-VOC
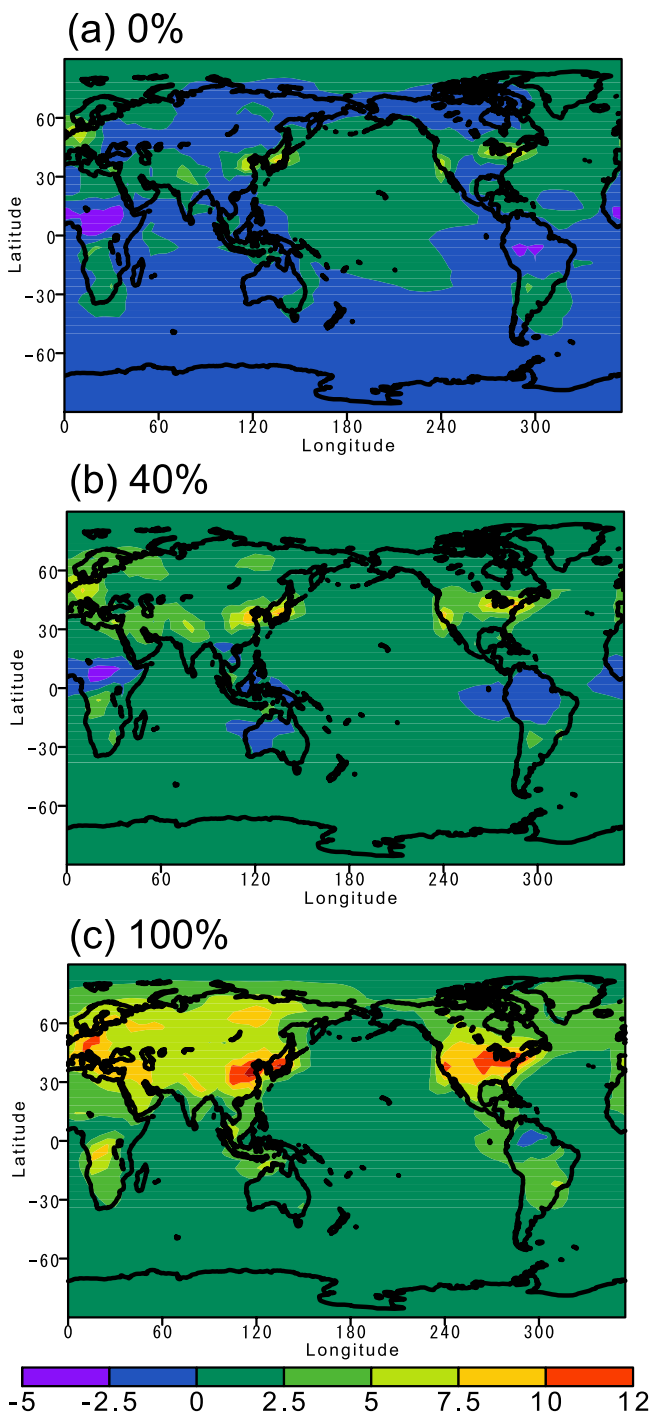
Figure 5. The change in surface O_3 mixing ratios (ppbv) in July due to the effects of a 5-K increase in temperature on the emission and chemical reaction rate coefficients for the assumption of (a) 0% recycling of NO_x from isoprene nitrates, (b) 40% recycling of NO_x from isoprene nitrates, and (c) 100% recycling of NO_x from isoprene nitrates.
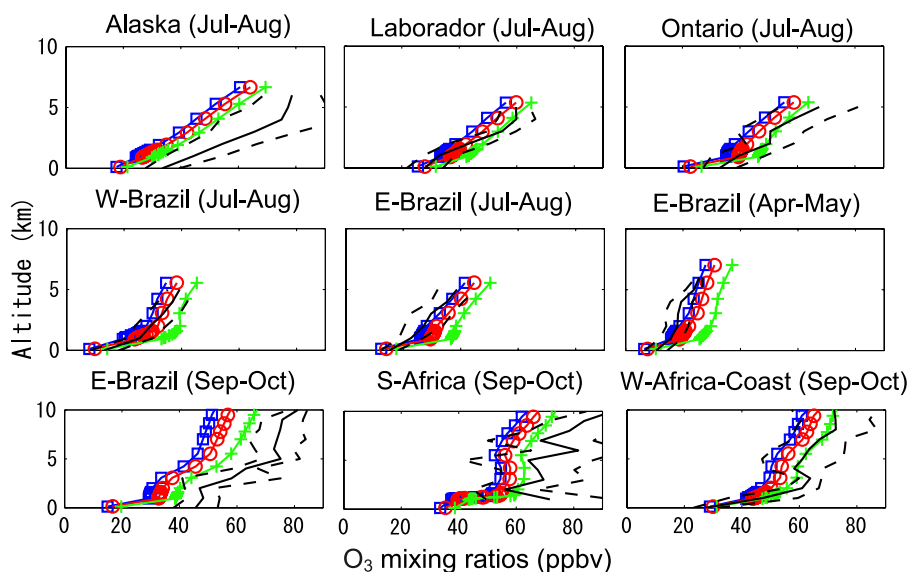
urban areas. The reasons for the specific model calibration should be elucidated before implementing it these calibrations in future predictions. In section 4.3.2.3, the correlation of O_3 with ΣANs is compared between model results and observations.

4.3. Comparison With Observations

[41] The performance of the model in simulating the observed O_3 and other intermediate species has been presented in earlier studies [*Rotman et al.*, 2004; *Ito et al.*,
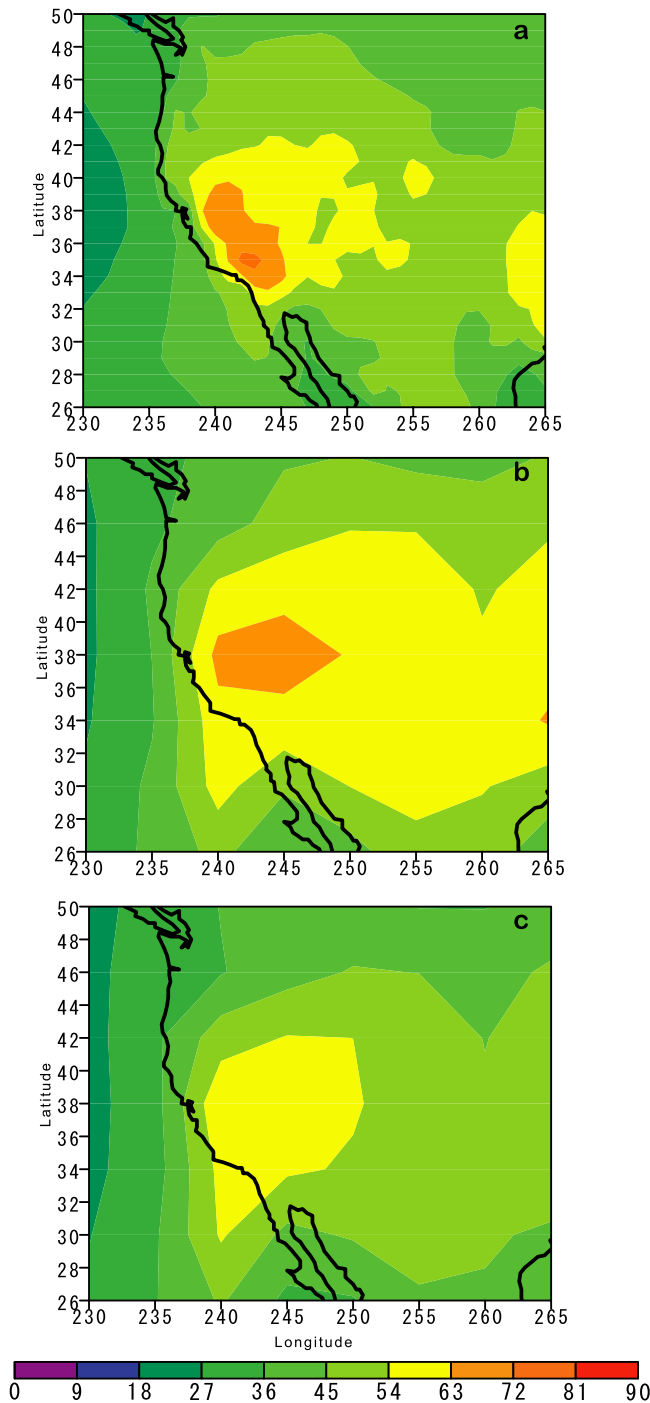
Figure 6. Ozone modeled surface mixing ratios (ppb) for (a) H_100, (b) L_100, and (c) L_40. All maps are monthly averages for July.

conditions because the artificial mixing of higher BVOC leads to more formation of ΣANs (more recycling of NO_x and thus more production of O_3) than actual partitioning into HNO_3. In this case, the decrease of NO_x availability for O_3 production with temperature in rural areas should not be related to BVOC emissions in rural areas but to those in

Figure 7. Comparison between measured O₃ [*Emmons et al.*, 2000] and model results at various sites. The blue lines with squares represent the mixing ratios of O₃ with 0% NOₓ recycling. The red lines with circles denote the mixing ratios of O₃ with 40% NOₓ recycling. The green lines with crosses show the mixing ratios of O₃ with 100% NOₓ recycling. Observations are indicated by the black lines. The black dashed lines show the standard deviations of measured values.

2007a]. *Ito et al.* [2007a] have shown the comparison between the model and observations for ΣPNs and ΣANs with different NOₓ recycling fractions for isoprene nitrates. In section 4.3.1, we provide some additional discussion on the comparison of O₃ mixing ratios with measurements. Further, the responses of O₃, OH and reactive nitrogen compounds to temperature changes are discussed in section 4.3.2.

4.3.1. Comparisons With Observed O₃

[42] In order to identify whether the changes in the NOₓ recycling fraction affect the agreement of the vertical profile between models and measurements, the average O₃ mixing ratios from the simulations with low, middle, and high NOₓ recycling fractions are compared with ambient measurements (Figure 7). The observational data set was compiled from field campaigns over selected regions and dates by *Emmons et al.* [2000].

[43] The uncertainty ranges in O₃ mixing ratios due to different NOₓ recycling fractions over tropical regions (10 ppbv) are larger than those at northern midlatitudes (8 ppbv) during summer. The ranges over East Brazil (14 ppbv) during the Amazonian forest fire season for September and October are larger than those for other seasons. The ranges are larger at higher altitudes (around 8 km) than those at lower altitudes around 2 km (10ppbv). *Ito et al.* [2007a] showed that the surface O₃ mixing ratios for these regions were sensitive to different emission estimates from biomass burning but that those at higher altitudes (around 8 km) were less sensitive. These results suggest that measurements in the FT over isoprene-rich locations in regions with high-NOₓ emissions may provide constraints on the NOₓ recycling fraction.

4.3.2. Comparison of Sensitivities to Temperature

[44] Even if models agree with the current O₃ measurements, it would not necessarily guarantee that the models could predict the future O₃ well, as we showed by examining the response of O₃ to temperature changes due to

different NOₓ recycling rates. However, the model should represent the response of O₃ to short-term changes before extrapolating it to long-term changes. The ability of models to predict the response of O₃ to short-term changes in temperature can be evaluated in part by examining how ambient concentrations of O₃ and other related species respond to day-to-day variations in temperature. It is well known that O₃ in polluted regions shows a strong correlation with temperature [e.g., *Sillman and Samson*, 1995]. Recently, *Day et al.* [2008] reported measurements for the variation of O₃ and various reactive nitrogen species with temperature at the University of California–Blodgett Forest Research Station (UC–BFRS) (1315 m above sea level, 38.9° N, 120.6° W) during the summer of 2001. This location is a forested in the Sierra foothills and is removed from immediate anthropogenic influence, but is strongly influenced by urban emissions from Sacramento (80 km to the northwest) and other urban centers in the San Joaquin valley. Here we examine the predicted correlations with temperatures from model simulations for the same time period in comparison with measured values. These day-to-day variations with temperature are largely influenced by changes in reaction rates and in biogenic emissions associated with temperature [e.g., *Steiner et al.*, 2006; *Day et al.*, 2008]. Correlations with temperature can also be influenced by meteorological patterns, such as correlations between winds, vertical diffusion or cloudiness with temperature [e.g., *Jacob et al.*, 1993], although *Day et al.* [2008] concluded that these had a relatively minor influence at UC–BFRS during the time period.

[45] Table 3 shows the response of O₃, OH, and the reactive nitrogen species to day-to-day temperature changes based on model results for low and high horizontal resolution with different NOₓ recycling fractions (L_0, L_40, H_40, and H_100) and those reported by *Day et al.* [2008] at UC–BFRS from June to September. *Day et al.*

Table 3. Model Results Compared With O_3 and Reactive Nitrogen Compounds Measured and OH Inferred From the Observations of Temperature Trends in the HNO_3/NO_2 Ratio at Blodgett Forest Research Station by *Day et al.* [2008][a]

	L_0	L_40	H_40	H_100	*Day et al.* [2008]
			Mean Value at 298 K		
O_3 (ppbv)	56	58	51	57	64
NO_x (ppbv)	0.92	0.98	0.24	0.35	0.7
NO_z (ppbv)	2.8	2.9	2.0	2.3	2.3
OH (10^6 molecules cm^{-3})	8.8	9.3	2.2	2.8	18
$\Sigma PNs/NO_z$	0.26	0.26	0.19	0.22	0.49
$\Sigma ANs/NO_z$	0.13	0.10	0.15	0.10	0.20
HNO_3/NO_z	0.61	0.64	0.66	0.68	0.42
HNO_3/NO_2	2.6	2.6	7.4	6.3	2.0
			Slope K^{-1}		
O_3 (ppbv)	+2.5	+2.8	+1.4	+2.0	+2.2
NO_x (ppbv)	+0.011	+0.015	+0.006	+0.015	−0.0007
NO_z (ppbv)	+0.11	+0.13	+0.11	+0.14	+0.036
OH (10^6 molecules cm^{-3})	−0.29	−0.27	−0.031	−0.008	+1.1
$\Sigma PNs/NO_z$	−0.014	−0.013	−0.019	−0.018	−0.023
$\Sigma ANs/NO_z$	+0.0037	+0.0022	−0.0001	−0.0009	+0.0036
HNO_3/NO_z	+0.0098	+0.011	+0.019	+0.019	+0.019
HNO_3/NO_2	+0.081	+0.084	+0.35	+0.22	+0.11

[a]The model results of L_0, L_40, H_40, and H_100 and the measurements are for 1200–1600 LT, 1 June to 30 September 2001.

[2008] observed the sum of gas-phase HNO_3 and thermally labile HNO_3 aerosols such as NH_4NO_3. However, *Day et al.* [2008] concluded that any aerosol NO_3^- in the region was nonvolatile and would not have been detected as part of their measurements of HNO_3. Similarly, *Day et al.* [2008] observed the sum of all alkyl and multifunctional nitrates present in the gas or aerosol phase. Thus we calculate the total alkyl nitrate in our model for comparison with their observations. The afternoon (1200–1600 LT) medians of O_3, OH, and the reactive nitrogen species are calculated for each day of summer 2001. The slope is calculated from a least squares fit to the median and the daily maximum temperature. The mean value for each species at 298 K is estimated from the function for each scenario. *Day et al.* [2008] excluded the observations on Saturday through Monday and days where trace gas species were influenced by forest fires from the measured values. We present here all days from the model results of L_0, L_40, H_40, and H_40, since we did not include weekday-weekend differences in emissions or event-specific forest fires in the model (Figures 8–10). Thus the total number of days included in our analysis (122) is larger than that for measured values (63).

4.3.2.1. ΣPNs, ΣANs, and HNO_3

[46] Comparisons between model results and measurements at the UC–BFRS site are difficult because the coarse horizontal resolution does not account for the distinctive local geography, in which anthropogenic emissions from urban sources are transported to the measurement site in a region with high-BVOC emissions. The model includes both the Sacramento urban area (80 km upwind from UC–BFRS) and the UC–BFRS site within the same horizontal grid for the low and middle resolutions but not for the high-resolution model ($1° \times 1°$). However, it is noteworthy that the ratios of the relatively long lived NO_x reaction products (ΣPNs, ΣANs, and HNO_3) to NO_z show variations with temperature that are comparable with measurements (Figure 8). The correlation coefficients of $\Sigma PNs/NO_z$ (0.46), $\Sigma ANs/NO_z$ (0.17), and HNO_3/NO_z (0.27) with temperature are comparable to that of *Day et al.* [2008] (0.52, 0.069, and 0.37, respectively). Despite the low R^2

values, Figure 8 shows that the regression lines capture the major patterns present in the data. The model slopes versus temperature are all statistically significant at a 95% confidence interval except for $\Sigma ANs/NO_z$, which shows a weak dependence on temperature in both the model and measurements. The match of the model trend to observed trend varies with the model simulation, but the H_40 trends versus temperature for $\Sigma PNs/NO_z$ (−0.02 ppb K^{-1}), $\Sigma ANs/NO_z$ (0.00 ppb K^{-1}), and HNO_3/NO_z (0.02 K^{-1}) are noticeably closer to the observed trends. The ratio of ΣPNs to NO_z decreases, the ratio of ΣANs to NO_z does not change, and the ratio of HNO_3 to NO_z increases with increasing temperature both in the model and in the measurements. The mixing ratios of NO_z in model are in good agreement (within 26%) with observations, while the ratios of ΣPNs, $\Sigma ANOs$, and HNO_3 to NO_z in the model differ significantly from the measured values at UC–BFRC. The model underestimates $\Sigma PNs/NO_z$ and $\Sigma ANs/NO_z$ but overestimates HNO_3/NO_z, possibly suggesting that the anthropogenic NO_x is more quickly converted to oxidized products by reactions with OH than by those with RO_2 under urban area conditions in the model where OH is high and BVOC emissions are low.

4.3.2.2. O_3

[47] The model scenarios also estimate that day-to-day ambient O_3 correlates with temperature ($R^2 = 0.55$ for L_0, 0.56 for L_40, 0.25 for H_40 and 0.34 for H_100) and that the rate of increase is comparable to the observed increase at UC–BFRC. The model scenarios that use a 0% NO_x recycling fraction in the low-resolution model and 100% NO_x recycling in the high-resolution model show increased O_3 (2.5 and 2.0 ppbv K^{-1}) with temperature that is comparable to the observed slope in O_3 versus temperature (2.2 ppbv K^{-1}). Our O_3 mixing ratios (58 ppbv at 298 K for L_40) are also in good agreement with the observations (Figure 8).

4.3.2.3. ΣANs and O_3

[48] *Horowitz et al.* [2007] found higher slope with higher NO_x recycling (100%; 257 O_3 per ΣANs) but lower slope with higher yield of isoprene nitrate (8%; 62 O_3 per
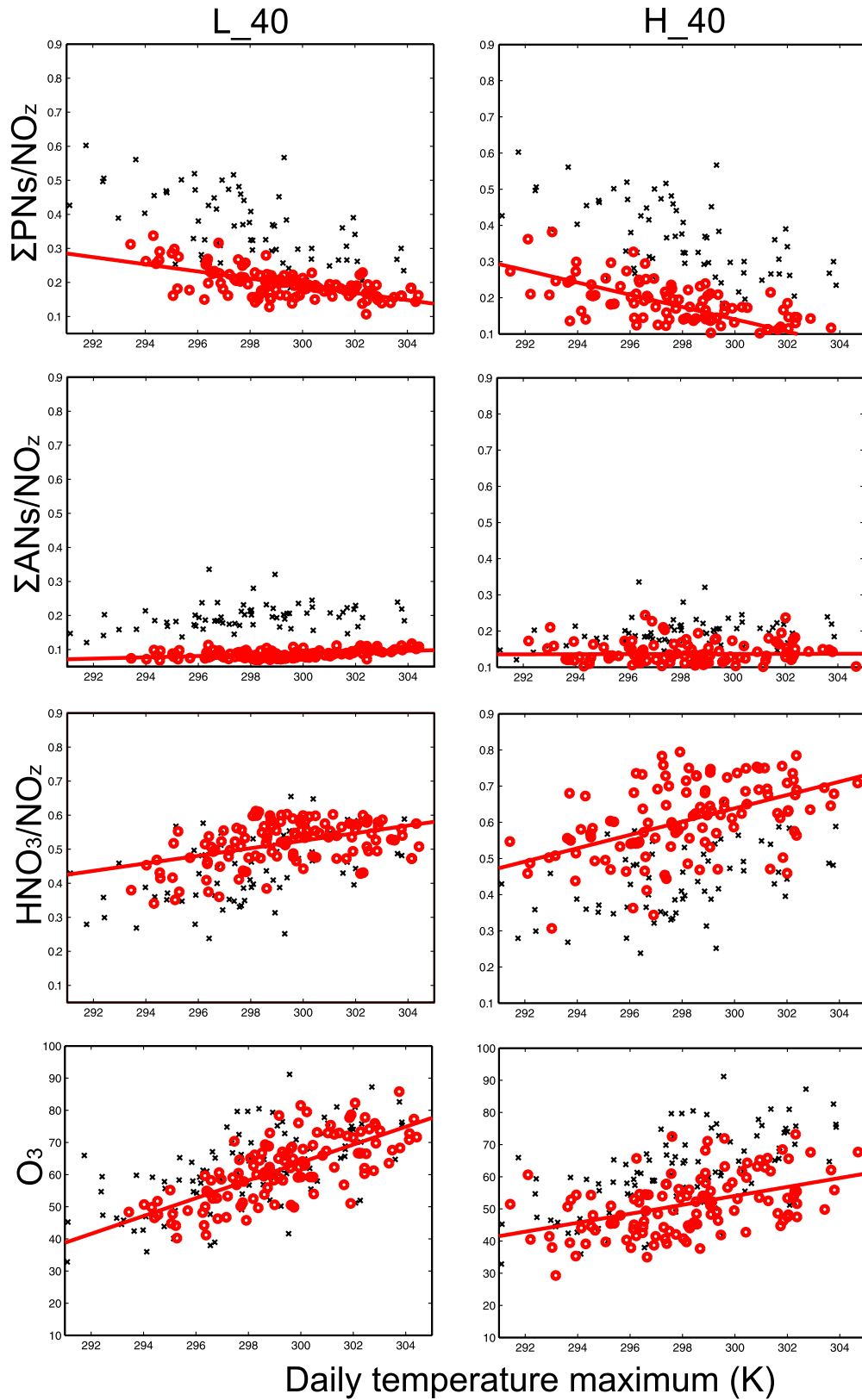
Figure 8. Modeled (red) and observed (black) $\Sigma PNs/NO_z$, $\Sigma ANs/NO_z$, HNO_3/NO_z, and O_3 versus daily maximum temperature (K) for 1200–1600 LT, June to September 2001 (L_40 and H_40 simulations) at UC–BFRS.
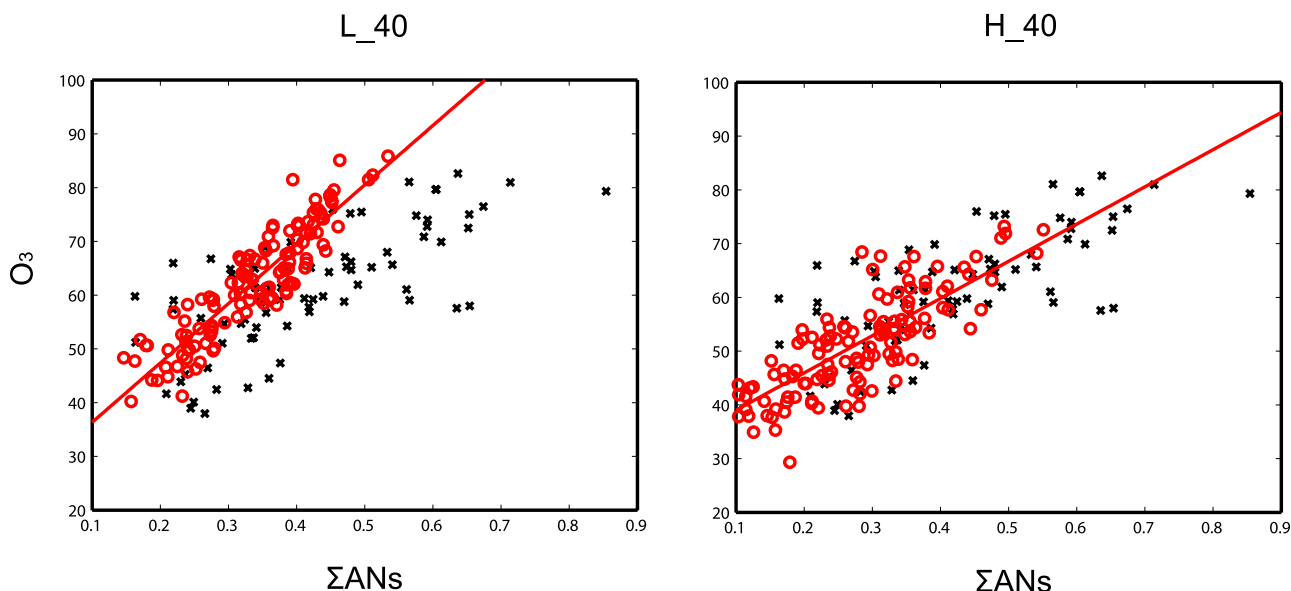
Figure 9.   Modeled (red) and observed (black) O_3 versus ΣANs for 1200–1600 LT, June to September 2001 (L_40 and H_40 simulations) at UC–BFRS.

ΣANs). Our results in the surface air using the high yield of isoprene nitrate show lower slope with higher resolution (106 for L_40 versus 69 for H_40) (Figure 9). The slope between model O_3 and ΣANs shows similar sensitivity to the model resolution as to NO_x recycling from isoprene nitrates (69 for H_40 versus 106 for H_100). These results suggest that the assumptions of higher yield of isoprene nitrate and higher NO_x recycling fractions using higher-resolution simulation might be able to match the slope of O_3 per ΣANs.
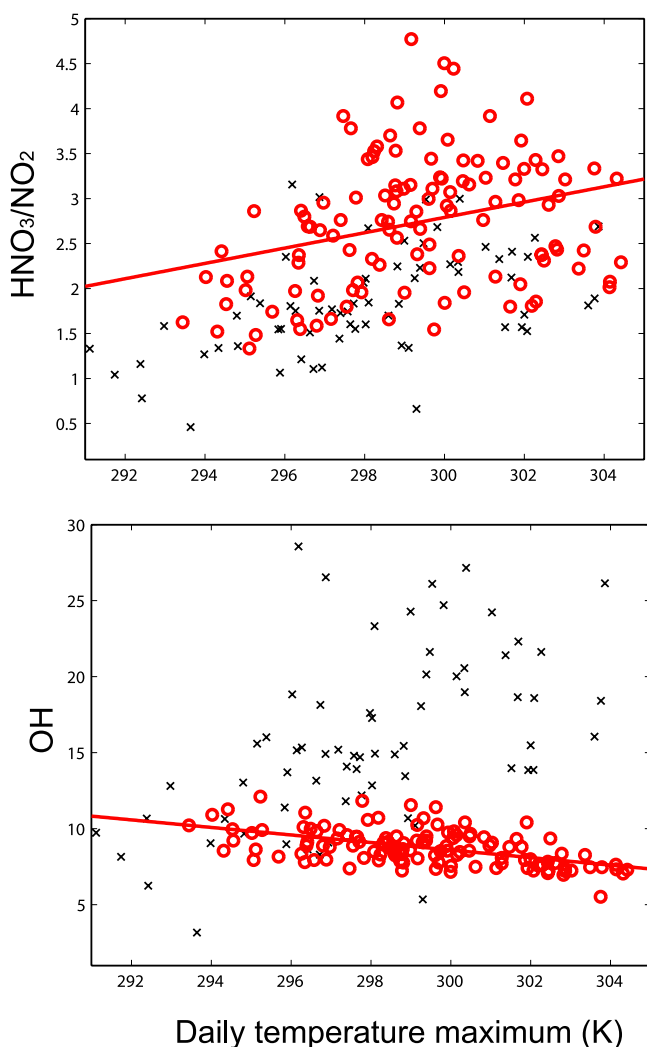
4.3.2.4. OH

[49]   Typically, models underestimate OH concentrations in regions with high-VOC and low-NO mixing ratios [e.g., *Carslaw et al.*, 2001; *Tan et al.*, 2001; *Thornton et al.*, 2002; *Karl et al.*, 2007; *Kuhn et al.*, 2007; *Farmer and Cohen*, 2008; *Ren et al.*, 2008]. A key question here with regard to the temperature dependency of OH is whether OH increases with temperature owing to the ozonolysis of unidentified reactive BVOC as a temperature-dependent source of OH in the atmosphere [*Kurpius and Goldstein*, 2003; *Di Carlo et al.*, 2004] or owing to the efficient OH recycling via HO_2 + RO_2 reactions which occur in an unpolluted low-NO_x environment [*Thornton et al.*, 2002; *Lelieveld et al.*, 2008; *Butler et al.*, 2008]. In the former case, the sensitivity of O_3 to the assumed NO_x recycling fraction may be less important, because the additional OH sources would partition anthropogenic NO_x into HNO_3 with warmer temperatures. In the latter case, the assumed NO_x recycling fraction can have a large influence on anthropogenic NO_x, but it depends on how much OH forms relative to BVOC and NO levels.

[50]   *Day et al.* [2008] infer that OH rapidly increases with temperature in the mixed layer, on the basis of the observed increase in the ratio of HNO_3/NO_2 with increasing temperature. The model OH concentrations in the high-resolution version ($2–3 \times 10^6$ molecules cm^{-3}) are lower than inferred value at UC–BFRC (18×10^6 molecules cm^{-3}).

The low OH at high resolution is probably due to the low NO_x (0.2–0.4 ppb). The measured NO_x (0.7 ppb) is influenced by transport of NO_x from urban source regions to the UC–BFRC site by a strong mountain/valley wind over the western slope of the Sierra Nevada [*Murphy et al.*, 2006]. In the low-resolution simulation, our OH (9×10^6 molecules cm^{-3}) is in better agreement with the inferred value than the model at the high resolution, probably because the conditions in the low-resolution version represent relatively high-NO_x conditions (0.98 ppb at 298 K for L_40), which are in much better agreement with the observations. In the low-resolution model simulations (Figure 10), OH in the afternoon is calculated to decrease with temperature (-0.27×10^6 molecules cm^{-3} K^{-1} for L_40), in contrast to the behavior of OH inferred. Thus one might argue that the additional OH required to match the inferred increase in OH with temperature might be explained by the ozonolysis of unidentified reactive BVOC as a temperature-dependent source of OH in the atmosphere [*Kurpius and Goldstein*, 2003; *Di Carlo et al.*, 2004]. However, the model results for HNO_3/NO_2 (2.6 at 298 K) and its increase with temperature (0.08 K^{-1}) are in good agreement with the measurements without the assumption of a temperature-dependent source of OH.

[51]   The increases in HNO_3 with temperature can be associated with changes in the PAN thermal equilibrium providing increased NO_2, which reacts with OH to form HNO_3. The increases in both OH and NO_2 versus temperature can be seen earlier in the day, but are no longer visible in the model afternoon values. A similar tendency appeared in the calculations reported by *Sillman and Samson* [1995]. The observed increase in HNO_3/NO_2 with temperature reported by *Day et al.* [2008] may also reflect increases in HNO_3 in upwind urban areas rather than changes in OH at the site. *Murphy et al.* [2006] suggested that the observed NO_y at noon at UC–BFRS reflected urban emissions during

Figure 10. Modeled (red) and observed/inferred (black) HNO_3/NO_2 and OH versus daily maximum temperature (K) for 1200–1600 LT, June to September 2001 (L_40 simulation) at UC–BFRS.

Sacramento urban plume using a Lagrangian model and VOC measurements.

[52] Finally, model results using the low- and high-resolution versions for July are also compared with measurements of isoprene, OH, and NO from three summer field campaigns: AEROBIC97 (39.9° N, 21.7° E), PROPHET98 (45.6° N, 84.7° W), and PMTACS-NY (44.4° N, 73.9° W) (Table 4). The model results at rural sites are in good agreement with the daytime peak OH levels in the Northern Hemisphere [*Carslaw et al.*, 2001; *Tan et al.*, 2001; *Ren et al.*, 2006]. These results might justify the predictability of the model at the rural sites to support our interpretation over isoprene-emitting regions near polluted source areas. On the other hand, *Butler et al.* [2008] have shown that the modeled OH concentrations over the three sites were too high with artificial OH recycling. Clearly, further work is needed to investigate the role of OH relative to BVOC and NO mixing ratios before the practical application of OH recycling to CTM.

5. Summary and Conclusions

[53] We investigated the effects of temperature changes (±5 K) on O_3 mixing ratios by examining changes in BVOC emissions and chemistry reaction rate coefficients. Our focus was to elucidate the relationship between the treatment of isoprene nitrates and the horizontal resolution in the model and to evaluate the ability of the model to predict temperature-dependent responses of O_3 and long-lived NO_x reaction products (ΣPNs, ΣANs, and HNO_3) on the basis of observed response.

[54] Global CTM calculations showed that the increases in the tropospheric O_3 burden as a result of the increases in BVOC, in particular isoprene (270–940 TgC a^{-1}), emissions associated with temperature increases strongly depended on the assumption of the amount of recycling of NO_x from isoprene nitrates (17–57 Tg for 0–100% NO_x recycling). Substantial differences in the global mean O_3 burden (40 Tg) were caused by the differences in the

the morning rush hour located 5–6 h upwind. As noted by *Day et al.* [2008] and *Farmer and Cohen* [2008], HNO_3 is produced more rapidly upwind where NO_2 mixing ratios are much higher [*Murphy et al.*, 2006]. Thus the overestimate of OH and its increase with temperature in the steady state calculation from the HNO_3/NO_2 ratio is probably associated with the content of the transported air (i.e., increased HNO_3 with temperature in the upwind urban areas). In this context, *Sillman and Samson* [1995] reported that OH and HNO_3/NO_2 both increase sharply with temperature in calculations for an urban location. Further, *Lelieveld et al.* [2008] and *Butler et al.* [2008] calculated an insignificant change in OH (±5%) during June, July, and August over this region when they changed the fraction of OH recycling associated with isoprene oxidation. Thus, at moderately high NO_x conditions, OH concentrations are not expected to increase significantly as a result of OH recycling. In this context it is noteworthy that our OH in the low-resolution model is in fairly good agreement with that of *Dillon et al.* [2002], who calculated OH (11 ± 5 × 10^6 molecules cm^{-3}) in the

Table 4. Measured OH Concentrations and Mixing Ratios of Isoprene and NO at Local Noon From Field Measurements Compared With Model Simulations[a]

	L_0	L_40	H_40	H_100	AEROBIC97
Isoprene[b]	0.59	0.52	1.9	1.6	1
NO[c]	33	43	85	113	<100
OH[c]	3.4	4.1	2.3	3.1	4
	L_0	L_40	H_40	H_100	PROPHET98
Isoprene[d]	0.58	0.51	2.2	1.7	2
NO[e]	148	157	40	60	<100
OH[e]	4.7	5.3	1.4	2.0	4
	L_0	L_40	H_40	H_100	PMTACS-NY
Isoprene[f]	0.93	0.85	2.0	1.6	<1
NO[f]	178	187	130	150	≈100
OH[f]	4.1	4.5	2.2	2.7	3

[a]Units are ×10^6 molecules cm^{-3} for OH concentrations, ppbv for mixing ratios of isoprene, and pptv for mixing ratios of NO.
[b]*Harrison et al.* [2001].
[c]*Carslaw et al.* [2001].
[d]*Apel et al.* [2002].
[e]*Tan et al.* [2001].
[f]*Ren et al.* [2006].

assumption of the amount of recycling of NO_x from isoprene nitrates between 0% and 100%. These differences were equivalent to the differences in the model resolution between the high resolution (302 Tg) and the low with the 40% NO_x recycling fraction (340 Tg). Our results in the surface air at a forested site in California showed lower slope with higher resolution (106 for L_40 versus 69 for H_40). The slope between model O_3 and ΣANs showed similar sensitivity to the model resolution as to NO_x recycling from isoprene nitrates (69 for H_40 versus 106 for H_100). The model versus measured slope might be used to infer the yield of isoprene nitrate and NO_x recycling fraction. However, our results indicate that the model slope and the recycling efficiencies of NO_x in a CTM are related to the isoprene nitrate chemistry as well as the grid resolution. It suggests that better agreement in the response of O_3 to temperature increases with observations could be achieved by using higher-resolution model with higher yield of isoprene nitrate and higher NO_x recycling fraction from isoprene nitrate.

[55] Model results have been compared with the observed responses in O_3 and reactive nitrogen compounds to temperature at a forested site in California observed by *Day et al.* [2008]. The model result showed a rapid increase in O_3 (2.0 ppb K^{-1}) and HNO_3/NO_z (0.02 K^{-1}), little change in $\Sigma ANs/NO_z$ (0.00 ppb K^{-1}) and a decrease in $\Sigma PNs/NO_z$ (-0.02 ppb K^{-1}) with increasing temperatures in the surface air. These compare closely with the measured variations, although the agreement varies with scenarios and species considered (see Table 3 and Figure 8). These results might justify the predictability of the model at the rural sites to support our interpretation over isoprene-emitting regions near polluted source areas. However, the interactions of terrestrial ecosystems with human activities and climate change are highly complex and the temperature sensitivities of O_3 may vary in different conditions. Further work is needed to provide constraints on the response of O_3 to temperature increases for a more accurate model prediction of effect of climate change on air quality.

References

Allen, D. J., and K. E. Pickering (2002), Evaluation of lightning flash rate parameterizations for use in a global chemical transport model, *J. Geophys. Res.*, 107(D23), 4711, doi:10.1029/2002JD002066.

Apel, E. C., et al. (2002), Measurement and interpretation of isoprene fluxes and isoprene, methacrolein, and methyl vinyl ketone mixing ratios at the PROPHET site during the 1998 Intensive, *J. Geophys. Res.*, 107(D3), 4034, doi:10.1029/2000JD000225.

Arneth, A., P. A. Miller, M. Scholze, T. Hickler, G. Schurgers, B. Smith, and I. C. Prentice (2007), CO_2 inhibition of global terrestrial isoprene emissions: Potential implications for atmospheric chemistry, *Geophys. Res. Lett.*, 34, L18813, doi:10.1029/2007GL030615.

Arneth, A., R. K. Monson, G. Schurgers, Ü. Niiemets, and P. I. Palmer (2008), Why are estimates of global terrestrial isoprene emissions so similar (and why is this not so for monoterpenes)?, *Atmos. Chem. Phys.*, 8, 4605–4620.

Atkinson, R., D. L. Baulch, R. A. Cox, J. N. Crowley, R. F. Hampson, R. G. Hynes, M. E. Jenkin, M. J. Rossi, and J. Troe (2004), Evaluated kinetic and photochemical data for atmospheric chemistry: Volume 1 - gas phase reactions of O_x, HO_x,, NO_x, and SO_x, species, *Atmos. Chem. Phys.*, 4, 1461–1738.

Bey, I., D. Jacob, R. Yantosca, J. Logan, B. Field, A. Fiore, Q. Li, H. Liu, L. Mickley, and M. Schultz (2001), Global modeling of tropospheric chemistry with assimilated meteorology: Model description and evaluation, *J. Geophys. Res.*, 106(D19), 23,073–23,096, doi:10.1029/2001JD000807.

Brasseur, G. P., J. T. Kiehl, J.-F. Müller, T. Schneider, C. Granier, X. Tie, and D. Hauglustaine (1998), Past and future changes in global tropospheric ozone: Impact on radiative forcing, *Geophys. Res. Lett.*, 25(20), 3807–3810, doi:10.1029/1998GL900013.

Brasseur, G. P., M. Schultz, C. Granier, M. Saunois, T. Diehl, M. Botzet, E. Roeckner, and S. Walters (2006), Impact of climate change on the future chemical composition of the global troposphere, *J. Clim.*, 19, 3932–3951, doi:10.1175/JCLI3832.1.

Butler, T. M., D. Taraborrelli, C. Brühl, H. Fischer, H. Harder, M. Martinez, J. Williams, M. G. Lawrence, and J. Lelieveld (2008), Improved simulation of isoprene oxidation chemistry with the ECHAM5/MESSy chemistry-climate model: Lessons from the GABRIEL airborne field campaign, *Atmos. Chem. Phys.*, 8, 4529–4546.

Byun, D., and K. L. Schere (2006), Review of the governing equations, computational algorithms, and other components of the Models-3 Community Multiscale Air Quality (CMAQ) modeling system, *Appl. Mech. Rev.*, 59, 51–77, doi:10.1115/1.2128636.

Carslaw, N., et al. (2001), OH and HO_2 radical chemistry in a forested region of north-western Greece, *Atmos. Environ.*, 35, 4725–4737, doi:10.1016/S1352-2310(01)00089-9.

Carter, W. P. L. (2000), Implementation of the SAPRC-99 chemical mechanism into the Models-3 framework, report, U. S. Environ. Prot. Agency, Washington, D. C.

Carter, W. P. L., A. M. Winer, K. R. Darnall, and J. N. Pitts (1979), Smog chamber studies of temperature effects in photochemical smog, *Environ. Sci. Technol.*, 13, 1094–1100, doi:10.1021/es60157a006.

Chen, X., D. Hulbert, and P. B. Shepson (1998), Measurement of the organic nitrate yield from OH reaction with isoprene, *J. Geophys. Res.*, 103(D19), 25,563–25,568, doi:10.1029/98JD01483.

Dawson, J. P., P. J. Adams, and S. N. Pandis (2007), Sensitivity of ozone to summertime climate in the eastern USA: A modeling case study, *Atmos. Environ.*, 41, 1494–1511, doi:10.1016/j.atmosenv.2006.10.033.

Day, D. A., M. B. Dillon, P. J. Wooldridge, J. A. Thornton, R. S. Rosen, E. C. Wood, and R. C. Cohen (2003), On alkyl nitrates, O_3, and the ''missing NO_y'', *J. Geophys. Res.*, 108(D16), 4501, doi:10.1029/2003JD003685.

Day, D. A., P. J. Wooldridge, and R. C. Cohen (2008), Observations of the effects of temperature on atmospheric HNO_3, ΣANs, ΣPNs, and NO_x: Evidence for a temperature dependent HO_x source, *Atmos. Chem. Phys.*, 8, 1867–1879.

Dentener, F., et al. (2006a), The global atmospheric environment for the next generation, *Environ. Sci. Technol.*, 40, 3586–3594, doi:10.1021/es0523845.

Dentener, F., et al. (2006b), Emissions of primary aerosol and precursor gases for the years 2000 and 1750 prescribed data-sets for AeroCom, *Atmos. Chem. Phys.*, 6, 4321–4344.

Di Carlo, P., et al. (2004), Missing OH reactivity in a forest: Evidence for unknown reactive biogenic VOCs, *Science*, 304, 722–725, doi:10.1126/science.1094392.

Dillon, M. B., M. S. Lamanna, G. W. Schade, A. H. Goldstein, and R. C. Cohen (2002), Chemical evolution of the Sacramento urban plume: Transport and oxidation, *J. Geophys. Res.*, 107(D5), 4045, doi:10.1029/2001JD000969.

Emmons, L. K., D. A. Hauglustaine, J.-F. Müller, M. A. Carroll, G. P. Brasseur, D. Brunner, J. Staehelin, V. Thouret, and A. Marenco (2000), Data composites of airborne observations of tropospheric ozone and its precursors, *J. Geophys. Res.*, 105, 20,497–20,538, doi:10.1029/2000JD900232.

Farmer, D. K., and R. C. Cohen (2008), Observations of HNO_3, ΣAN, ΣPN and NO_2 fluxes: Evidence for rapid HO_x chemistry within a pine forest canopy, *Atmos. Chem. Phys.*, 8, 3899–3917.

Fehsenfeld, F. C., et al. (2006), International Consortium for Atmospheric Research on Transport and Transformation (ICARTT): North America to Europe—Overview of the 2004 summer field study, *J. Geophys. Res.*, 111, D23S01, doi:10.1029/2006JD007829.

Feng, Y., and J. E. Penner (2007), Global modeling of nitrate and ammonium: Interaction of aerosols and tropospheric chemistry, *J. Geophys. Res.*, 112, D01304, doi:10.1029/2005JD006404.

Fiore, A. M., D. J. Jacob, R. Mathur, and R. V. Martin (2003), Application of empirical orthogonal functions to evaluate ozone simulations with

regional and global models, *J. Geophys. Res.*, *108*(D14), 4431, doi:10.1029/2002JD003151.

Fiore, A. M., L. W. Horowitz, D. W. Purves, H. Levy II, M. J. Evans, Y. Wang, Q. Li, and R. M. Yantosca (2005), Evaluating the contribution of changes in isoprene emissions to surface ozone trends over the eastern United States, *J. Geophys. Res.*, *110*, D12303, doi:10.1029/2004JD005485.

Fiore, A. M., L. W. Horowitz, E. J. Dlugokencky, and J. J. West (2006), Impact of meteorology and emissions on methane trends, 1990–2004, *Geophys. Res. Lett.*, *33*, L12809, doi:10.1029/2006GL026199.

Gery, M. W., G. Z. Whitten, J. P. Killus, and M. C. Dodge (1989), A photochemical kinetics mechanism for urban and regional scale computer modeling, *J. Geophys. Res.*, *94*, 12,925–12,956, doi:10.1029/JD094iD10p12925.

Giacopelli, P., K. Ford, C. Espada, and P. B. Shepson (2005), Comparison of the measured and simulated isoprene nitrate distributions above a forest canopy, *J. Geophys. Res.*, *110*, D01304, doi:10.1029/2004JD005123.

Giglio, L., I. Csiszar, and C. O. Justice (2006), Global distribution and seasonality of active fires as observed with the Terra and Aqua Moderate Resolution Imaging Spectroradiometer (MODIS) sensors, *J. Geophys. Res.*, *111*, G02016, doi:10.1029/2005JG000142.

Guenther, A., et al. (1995), A global model of natural volatile organic compound emissions, *J. Geophys. Res.*, *100*, 8873–8892, doi:10.1029/94JD02950.

Guenther, A., B. Baugh, G. Brasseur, J. Greenberg, P. Harley, L. Klinger, D. Serca, and L. Vierling (1999), Isoprene emission estimates and uncertainties for the central African EXPRESSO study domain, *J. Geophys. Res.*, *104*, 30,625–30,639, doi:10.1029/1999JD900391.

Guenther, A., T. Karl, P. Harley, C. Wiedinmyer, P. I. Palmer, and C. Geron (2006), Estimates of global terrestrial isoprene emissions using MEGAN (Model of Emissions of Gases and Aerosols from Nature), *Atmos. Chem. Phys.*, *6*, 3181–3210.

Harrison, D., et al. (2001), Ambient isoprene and monoterpene concentrations in a Greek fir (*Abies Borisii-regis*) forest: Reconciliation with emissions measurements and effects on measured OH concentrations, *Atmos. Environ.*, *35*, 4699–4711, doi:10.1016/S1352-2310(01)00091-7.

Hauglustaine, D. A., J. Lathière, S. Szopa, and G. A. Folberth (2005), Future tropospheric ozone simulated with a climate-chemistry-biosphere model, *Geophys. Res. Lett.*, *32*, L24807, doi:10.1029/2005GL024031.

Heald, C. L., M. J. Wilkinson, R. K. Monson, C. A. Alo, G. Wang, and A. Guenther (2009), Response of isoprene emission to ambient CO_2 changes and implications for global budgets, *Global Change Biol.*, in press.

Herman, J. R., P. K. Bhartia, O. Torres, C. Hsu, C. Seftor, and E. Celarier (1997), Global distribution of UV-absorbing aerosols from Nimbus-7/ TOMS data, *J. Geophys. Res.*, *102*, 16,911–16,922, doi:10.1029/96JD03680.

Hogrefe, C., B. Lynn, K. Civerolo, J.-Y. Ku, J. Rosenthal, C. Rosenzweig, R. Goldberg, S. Gaffin, K. Knowlton, and P. L. Kinney (2004), Simulating changes in regional air pollution over the eastern United States due to changes in global and regional climate and emissions, *J. Geophys. Res.*, *109*, D22301, doi:10.1029/2004JD004690.

Horowitz, L. W., J. Liang, G. M. Gardner, and D. J. Jacob (1998), Export of reactive nitrogen from North America during summertime: Sensitivity to hydrocarbon chemistry, *J. Geophys. Res.*, *103*(D11), 13,451–13,476, doi:10.1029/97JD03142.

Horowitz, L. W., et al. (2003), A global simulation of tropospheric ozone and related tracers: Description and evaluation of MOZART, version 2, *J. Geophys. Res.*, *108*(D24), 4784, doi:10.1029/2002JD002853.

Horowitz, L. W., A. M. Fiore, G. P. Milly, R. C. Cohen, A. Perring, P. J. Wooldridge, P. G. Hess, L. K. Emmons, and J.-F. Lamarque (2007), Observational constraints on the chemistry of isoprene nitrates over the eastern United States, *J. Geophys. Res.*, *112*, D12S08, doi:10.1029/2006JD007747.

Houweling, S., F. Dentener, and J. Lelieveld (1998), The impact of non-methane hydrocarbon compounds on tropospheric photochemistry, *J. Geophys. Res.*, *103*(D9), 10,673–10,696, doi:10.1029/97JD03582.

Ito, A., and J. E. Penner (2005), Historical emissions of carbonaceous aerosols from biomass and fossil fuel burning for the period 1870–2000, *Global Biogeochem. Cycles*, *19*, GB2028, doi:10.1029/2004GB002374.

Ito, A., S. Sillman, and J. E. Penner (2007a), Effects of additional non-methane volatile organic compounds, organic nitrates, and direct emissions of oxygenated organic species on global tropospheric chemistry, *J. Geophys. Res.*, *112*, D06309, doi:10.1029/2005JD006556.

Ito, A., K. Sudo, H. Akimoto, S. Sillman, and J. E. Penner (2007b), Global modeling analysis of tropospheric ozone and its radiative forcing from biomass burning emissions in the twentieth century, *J. Geophys. Res.*, *112*, D24307, doi:10.1029/2007JD008745.

Ito, A., A. Ito, and H. Akimoto (2007c), Seasonal and interannual variations in CO and BC emissions from open biomass burning in Southern Africa during 1998–2005, *Global Biogeochem. Cycles*, *21*, GB2011, doi:10.1029/2006GB002848.

Ito, A., et al. (2008), Can we reconcile differences in estimates of carbon fluxes from land-use change and forestry for the 1990s?, *Atmos. Chem. Phys.*, *8*, 3291–3310.

Jacob, D. J., J. A. Logan, G. M. Gardner, R. M. Yevich, C. M. Spivakovsky, and S. C. Wofsy (1993), Factors regulating ozone over the United States and its export to the global atmosphere, *J. Geophys. Res.*, *98*(D8), 14,817–14,826, doi:10.1029/98JD01224.

Jacob, D. J., et al. (2005), Global budget of methanol: Constraints from atmospheric observations, *J. Geophys. Res.*, *110*, D08303, doi:10.1029/2004JD005172.

Johnson, C. E., W. J. Collins, D. S. Stevenson, and R. G. Derwent (1999), Relative roles of climate and emissions changes on future tropospheric oxidant concentrations, *J. Geophys. Res.*, *104*(D15), 18,631–18,645, doi:10.1029/1999JD900204.

Karl, T., A. Guenther, R. J. Yokelson, J. Greenberg, M. Potosnak, D. R. Blake, and P. Artaxo (2007), The tropical forest and fire emissions experiment: Emission, chemistry, and transport of biogenic volatile organic compounds in the lower atmosphere over Amazonia, *J. Geophys. Res.*, *112*, D18302, doi:10.1029/2007JD008539.

Kuhn, U., et al. (2007), Isoprene and monoterpene fluxes from Central Amazonian rainforest inferred from tower-based and airborne measurements, and implications on the atmospheric chemistry and the local carbon budget, *Atmos. Chem. Phys.*, *7*, 2855–2879.

Kunkel, K. E., et al. (2008), Sensitivity of future ozone concentrations in the northeast USA to regional climate change, *Mitigation Adaptation Strategies Global Change*, *13*, 597–606, doi:10.1007/s11027-007-9137-y.

Kurpius, M. R., and A. H. Goldstein (2003), Gas-phase chemistry dominates O_3 loss to a forest, implying a source of aerosols and hydroxyl radicals to the atmosphere, *Geophys. Res. Lett.*, *30*(7), 1371, doi:10.1029/2002GL016785.

Lathière, J., D. A. Hauglustaine, N. De Noblet-Ducoudré, G. Krinner, and G. A. Folberth (2005), Past and future changes in biogenic volatile organic compound emissions simulated with a global dynamic vegetation model, *Geophys. Res. Lett.*, *32*, L20818, doi:10.1029/2005GL024164.

Lathière, J., D. A. Hauglustaine, A. D. Friend, N. De Noblet-Ducoudré, N. Viovy, and G. A. Folberth (2006), Impact of climate variability and land use changes on global biogenic volatile organic compound emissions, *Atmos. Chem. Phys.*, *6*, 2129–2146.

Lelieveld, J., et al. (2002), Global air pollution crossroads over the Mediterranean, *Science*, *298*, 794–799, doi:10.1126/science.1075457.

Lelieveld, J., et al. (2008), Atmospheric oxidation capacity sustained by a tropical forest, *Nature*, *452*, 737–740, doi:10.1038/nature06870.

Li, Q., et al. (2001), A tropospheric ozone maximum over the Middle East, *Geophys. Res. Lett.*, *28*(17), 3235–3238, doi:10.1029/2001GL013134.

Liang, J., and M. Z. Jacobson (2000), Effects of subgrid segregation on ozone production efficiency in a chemical model, *Atmos. Environ.*, *34*, 2975–2982, doi:10.1016/S1352-2310(99)00520-8.

Liu, S. C., M. Trainer, F. C. Fehsenfeld, D. D. Parrish, E. J. Williams, D. W. Fahey, G. Hubler, and P. C. Murphy (1987), Ozone production in the rural troposphere and the implications for regional and global ozone distributions, *J. Geophys. Res.*, *92*(D4), 4191–4207, doi:10.1029/JD092iD04p04191.

Liu, X., J. E. Penner, and M. Herzog (2005), Global modeling of aerosol dynamics: Model description, evaluation, and interactions between sulfate and nonsulfate aerosols, *J. Geophys. Res.*, *110*, D18206, doi:10.1029/2004JD005674.

McKeen, S. A., E.-Y. Hsie, and S. C. Liu (1991), A study of the dependence of rural ozone on ozone precursors in the eastern United States, *J. Geophys. Res.*, *96*(D8), 15,377–15,394, doi:10.1029/91JD01282.

McLinden, C., S. Olsen, B. Hannegan, O. Wild, M. Prather, and J. Sundet (2000), Stratospheric ozone in 3-D models: A simple chemistry and the cross-tropopause flux, *J. Geophys. Res.*, *105*(D11), 14,653–14,666, doi:10.1029/2000JD900124.

Mortlock, A. M., and R. Van Alstyne (1998), Military, charter, unreported domestic traffic and general aviation: 1976, 1984, 1992, and 2015 emission scenarios, *NASA CR- 1998–207639*, Natl. Aeronaut. and Space Admin., Washington, D. C.

Müller, J.-F., T. Stavrakou, S. Wallens, I. De Smedt, M. Van Roozendael, M. J. Potosnak, J. Rinne, B. Munger, A. Goldstein, and A. B. Guenther (2008), Global isoprene emissions estimated using MEGAN, ECMWF analyses and a detailed canopy environment model, *Atmos. Chem. Phys.*, *8*, 1329–1341.

Murazaki, K., and P. Hess (2006), How does climate change contribute to surface ozone change over the United States?, *J. Geophys. Res.*, *111*, D05301, doi:10.1029/2005JD005873.

Murphy, J. G., A. Day, P. A. Cleary, P. J. Wooldridge, and R. C. Cohen (2006), Observations of the diurnal and seasonal trends in nitrogen oxides in the western Sierra Nevada, *Atmos. Chem. Phys.*, *6*, 5321–5338.

Olszyna, K. J., M. Luria, and J. F. Meagher (1997), The correlation of temperature and rural ozone levels in southeastern USA, *Atmos. Environ.*, *31*, 3011–3022, doi:10.1016/S1352-2310(97)00097-6.

O'Sullivan, D. W., M. Lee, B. C. Noone, and B. G. Heikes (1996), Henry's law constant determinations for hydrogen peroxide, methyl hydroperoxide, hydroxymethyl hydroperoxide, ethyl hydroperoxide, and peroxyacetic acid, *J. Phys. Chem.*, *100*, 3241–3247, doi:10.1021/jp951168n.

Palmer, P. I., et al. (2006), Quantifying the seasonal and interannual variability of North American isoprene emissions using satellite observations of the formaldehyde column, *J. Geophys. Res.*, *111*, D12315, doi:10.1029/2005JD006689.

Paulot, F., J. D. Crounse, H. G. Kjaergaard, J. H. Kroll, J. H. Seinfeld, and P. O. Wennberg (2009), Isoprene photooxidation: New insights into the production of acids and organic nitrates, *Atmos. Chem. Phys.*, *9*, 1479–1501.

Paulson, S. E., and J. H. Seinfeld (1992), Development and evaluation of a photooxidation mechanism for isoprene, *J. Geophys. Res.*, *97*(D18), 20,703–20,715.

Pegoraro, E., A. Rey, G. Barron-Gafford, R. Monson, Y. Malhi, and R. Murthy (2005), The interacting effects of elevated atmospheric CO_2 concentration, drought and leaf-to-air vapour pressure deficit on ecosystem isoprene fluxes, *Oecologia*, *146*, 120–129, doi:10.1007/s00442-005-0166-5.

Perring, A. E., et al. (2009), Airborne observations of total $RONO_2$: New constraints on the yield and lifetime of isoprene nitrates, *Atmos. Chem. Phys.*, *9*, 1451–1463.

Pickering, K. E., Y. Wang, W.-K. Tao, C. Price, and J.-F. Müller (1998), Vertical distributions of lightning NO_x for use in regional and global chemical transport models, *J. Geophys. Res.*, *103*(D23), 31,203–31,216, doi:10.1029/98JD02651.

Pöschl, U., R. von Kuhlmann, N. Poisson, and P. J. Crutzen (2000), Development and intercomparison of condensed isoprene oxidation mechanisms for global atmospheric modeling, *J. Atmos. Chem.*, *37*, 29–52, doi:10.1023/A:1006391009798.

Prather, M., et al. (2003), Fresh air in the 21st century?, *Geophys. Res. Lett.*, *30*(2), 1100, doi:10.1029/2002GL016285.

Racherla, P. N., and P. J. Adams (2006), Sensitivity of global tropospheric ozone and fine particulate matter concentrations to climate change, *J. Geophys. Res.*, *111*, D24103, doi:10.1029/2005JD006939.

Racherla, P. N., and P. J. Adams (2008), The response of surface ozone to climate change over the eastern United States, *Atmos. Chem. Phys.*, *8*, 871–885.

Ren, X., et al. (2006), OH, HO_2, and OH reactivity during the PMTACS–NY Whiteface Mountain 2002 campaign: Observations and model comparison, *J. Geophys. Res.*, *111*, D10S03, doi:10.1029/2005JD006126.

Ren, X., et al. (2008), HO_x chemistry during INTEX-A 2004: Observation, model calculation, and comparison with previous studies, *J. Geophys. Res.*, *113*, D05310, doi:10.1029/2007JD009166.

Rosenstiel, T. N., M. J. Potosnak, K. L. Griffin, R. Fall, and R. K. Monson (2003), Increased CO_2 uncouples growth from isoprene emission in an agriforest ecosystem, *Nature*, *421*, 256–259, doi:10.1038/nature01312.

Rotman, D. A., et al. (2004), IMPACT, the LLNL 3-D global atmospheric chemical transport model for the combined troposphere and stratosphere: Model description and analysis of ozone and other trace gases, *J. Geophys. Res.*, *109*, D04303, doi:10.1029/2002JD003155.

Sander, R., et al. (2006), Chemical kinetics and photochemical data for use in atmospheric studies, *Eval. 15, JPL Publ. 06–2*, Jet Propul. Lab., Pasadena, Calif.

Sanderson, M. G., C. D. Jones, W. J. Collins, C. E. Johnson, and R. G. Derwent (2003), Effect of climate change on isoprene emissions and surface ozone levels, *Geophys. Res. Lett.*, *30*(18), 1936, doi:10.1029/2003GL017642.

Schubert, S. D., R. B. Rood, and J. Pfaendtner (1993), An assimilated data set for Earth Science applications, *Bull. Am. Meteorol. Soc.*, *74*, 2331–2342, doi:10.1175/1520-0477(1993)074<2331:AADFES>2.0.CO;2.

Schwartz, S. E., and W. H. White (1981), Solubility equilibria of the nitrogen oxides and oxyacids in dilute aqueous solution, in *Advances in Environmental Science and Engineering*, vol. 4, edited by J. R. Pfafflin and E. N. Ziegler, pp. 1–45, Gordon and Breach, New York.

Sillman, S., and P. J. Samson (1995), Impact of temperature on oxidant photochemistry in urban, polluted rural, and remote environments, *J. Geophys. Res.*, *100*(D6), 11,497–11,508, doi:10.1029/94JD02146.

Sillman, S., J. A. Logan, and S. C. Wofsy (1990), A regional scale model for ozone in the United States with subgrid representation of urban and power plant plumes, *J. Geophys. Res.*, *95*(D5), 5731–5748, doi:10.1029/JD095iD05p05731.

Singh, H. B., et al. (1998), Latitudinal distribution of reactive nitrogen in the free troposphere over the Pacific Ocean in late winter/early spring, *J. Geophys. Res.*, *103*(D21), 28,237–28,247, doi:10.1029/98JD01891.

Singh, H., et al. (2000), Distribution and fate of selected oxygenated organic species in the troposphere and lower stratosphere over the Atlantic, *J. Geophys. Res.*, *105*(D3), 3795–3806, doi:10.1029/1999JD900779.

Singh, H. B., W. H. Brune, J. H. Crawford, D. J. Jacob, and P. B. Russell (2006), Overview of the summer 2004 Intercontinental Chemical Transport Experiment–North America (INTEX-A), *J. Geophys. Res.*, *111*, D24S01, doi:10.1029/2006JD007905.

Sprengnether, M., K. L. Demerjian, N. M. Donahue, and J. G. Anderson (2002), Product analysis of the OH oxidation of isoprene and 1,3-butadiene in the presence of NO, *J. Geophys. Res.*, *107*(D15), 4268, doi:10.1029/2001JD000716.

Steiner, A. L., S. Tonse, R. C. Cohen, A. H. Goldstein, and R. A. Harley (2006), Influence of future climate and emissions on regional air quality in California, *J. Geophys. Res.*, *111*, D18303, doi:10.1029/2005JD006935.

Stevenson, D. S., C. E. Johnson, W. J. Collins, R. G. Derwent, and J. M. Edwards (2000), Future estimates of tropospheric ozone radiative forcing and methane turnover: The impact of climate change, *Geophys. Res. Lett.*, *27*(14), 2073–2076, doi:10.1029/1999GL010887.

Stevenson, D. S., et al. (2006), Multimodel ensemble simulations of present-day and near-future tropospheric ozone, *J. Geophys. Res.*, *111*, D08301, doi:10.1029/2005JD006338.

Sutkus, D. J., S. L. Baughcum, and D. P. DuBois (2001), Scheduled civil aircraft emission inventories for 1999: Database development and analysis, *NASA CR-2001–211216*, NASA, Washington, D. C.

Tagaris, E., K. Manomaiphiboon, K.-J. Liao, L. R. Leung, J.-H. Woo, S. He, P. Amar, and A. G. Russell (2007), Impacts of global climate change and emissions on regional ozone and fine particulate matter concentrations over the United States, *J. Geophys. Res.*, *112*, D14312, doi:10.1029/2006JD008262.

Tan, D., et al. (2001), HO_x budgets in a deciduous forest: Results from the PROPHET summer 1998 campaign, *J. Geophys. Res.*, *106*(D20), 24,407–24,427, doi:10.1029/2001JD900016.

Tao, Z., S. M. Larson, D. J. Wuebbles, A. Williams, and M. Caughey (2003), A summer simulation of biogenic contributions to ground-level ozone over the continental United States, *J. Geophys. Res.*, *108*(D14), 4404, doi:10.1029/2002JD002945.

Tao, Z., A. Williams, H.-C. Huang, M. Caughey, and X.-Z. Liang (2007), Sensitivity of U.S. surface ozone to future emissions and climate changes, *Geophys. Res. Lett.*, *34*, L08811, doi:10.1029/2007GL029455.

Thornton, J. A., et al. (2002), Ozone production rates as a function of NO_x abundances and HO_x production rates in the Nashville urban plume, *J. Geophys. Res.*, *107*(D12), 4146, doi:10.1029/2001JD000932.

von Kuhlmann, R., M. G. Lawrence, U. Pöschl, and P. J. Crutzen (2004), Sensitivities in global scale modeling of isoprene, *Atmos. Chem. Phys.*, *4*, 1–17.

Wang, Y., D. J. Jacob, and J. A. Logan (1998), Global simulation of tropospheric O_3-NO_x-hydrocarbon chemistry: 1. Model formulation, *J. Geophys. Res.*, *103*(D9), 10,713–10,725, doi:10.1029/98JD00158.

Wiedinmyer, C., X. X. Tie, A. Guenther, R. Neilson, and C. Granier (2006), Future changes in biogenic isoprene emissions: How might they affect regional and global atmospheric chemistry?, *Earth Interact.*, *10*, 1–19, doi:10.1175/EI174.1.

Wild, O. (2007), Modelling the global tropospheric ozone budget: Exploring the variability in current models, *Atmos. Chem. Phys.*, *7*, 2643–2660.

Wild, O., and M. J. Prather (2006), Global tropospheric ozone modeling: Quantifying errors due to grid resolution, *J. Geophys. Res.*, *111*, D11305, doi:10.1029/2005JD006605.

Wild, O., P. Pochanart, and H. Akimoto (2004), Trans-Eurasian transport of ozone and its precursors, *J. Geophys. Res.*, *109*, D11302, doi:10.1029/2003JD004501.

Wu, S., L. J. Mickley, D. J. Jacob, J. A. Logan, R. M. Yantosca, and D. Rind (2007), Why are there large differences between models in global budgets of tropospheric ozone?, *J. Geophys. Res.*, *112*, D05302, doi:10.1029/2006JD007801.

Wu, S., L. J. Mickley, E. M. Leibensperger, D. J. Jacob, D. Rind, and D. G. Streets (2008), Effects of 2000–2050 global change on ozone air quality in the United States, *J. Geophys. Res.*, *113*, D06302, doi:10.1029/2007JD008917.

Yan, X., T. Ohara, and H. Akimoto (2005), Statistical modeling of global soil NO_x emissions, *Global Biogeochem. Cycles*, *19*, GB3019, doi:10.1029/2004GB002276.

Zeng, G., J. A. Pyle, and P. J. Young (2008), Impact of climate change on tropospheric ozone and its global budgets, *Atmos. Chem. Phys.*, *8*, 369–387.

Zhang, Y., X.-M. Hu, L. R. Leung, and W. I. Gustafson Jr. (2008), Impacts of regional climate change on biogenic emissions and air quality, *J. Geophys. Res.*, *113*, D18310, doi:10.1029/2008JD009965.

Zhu, Y. Q., R. Todling, J. Guo, S. E. Cohn, I. M. Navon, and Y. Yang (2003), The GEOS-3 retrospective data assimilation system: The 6-hour lag case, *Mon. Weather Rev.*, *131*(9), 2129–2150, doi:10.1175/1520-0493(2003)131<2129:TGRDAS>2.0.CO;2.

_____

A. Ito (corresponding author), Frontier Research Center for Global Change, Japan Agency for Marine-Earth Science and Technology (JAMSTEC), 3173-25, Showa-machi, Yokohama 236-0001, Japan. (akinorii@jamstec.go.jp)

J. E. Penner and S. Sillman, Department of Atmospheric, Oceanic, and Space Sciences, University of Michigan, Ann Arbor, MI 48109, USA.